TU/e EINDHOVEN UNIVERSITY OF TECHNOLOGY

Connectivity percolation of polydisperse anisotropic nanofillers

Citation for published version (APA):
Otten, R. H. J., & Schoot, van der, P. P. A. M. (2011). Connectivity percolation of polydisperse anisotropic nanofillers. *Journal of Chemical Physics*, *134*(9), 094902-1/15. Article 094902. https://doi.org/10.1063/1.3559004

DOI:
10.1063/1.3559004

Document status and date:
Published: 01/01/2011

Document Version:
Publisher's PDF, also known as Version of Record (includes final page, issue and volume numbers)

Please check the document version of this publication:

• A submitted manuscript is the version of the article upon submission and before peer-review. There can be important differences between the submitted version and the official published version of record. People interested in the research are advised to contact the author for the final version of the publication, or visit the DOI to the publisher's website.
• The final author version and the galley proof are versions of the publication after peer review.
• The final published version features the final layout of the paper including the volume, issue and page numbers.

Link to publication

General rights
Copyright and moral rights for the publications made accessible in the public portal are retained by the authors and/or other copyright owners and it is a condition of accessing publications that users recognise and abide by the legal requirements associated with these rights.

• Users may download and print one copy of any publication from the public portal for the purpose of private study or research.
• You may not further distribute the material or use it for any profit-making activity or commercial gain
• You may freely distribute the URL identifying the publication in the public portal.

If the publication is distributed under the terms of Article 25fa of the Dutch Copyright Act, indicated by the "Taverne" license above, please follow below link for the End User Agreement:

www.tue.nl/taverne

Take down policy
If you believe that this document breaches copyright please contact us at:

openaccess@tue.nl

providing details and we will investigate your claim.

Download date: 03. Nov. 2024

Connectivity percolation of polydisperse anisotropic nanofillers

Ronald H. J. Otten[1,2,a] and Paul van der Schoot[1,3]
[1]*Theory of Polymers and Soft Matter and Eindhoven Polymer Laboratories, Eindhoven University of Technology, P.O. Box 513, 5600 MB Eindhoven, The Netherlands*
[2]*Dutch Polymer Institute, P.O. Box 902, 5600 AX Eindhoven, The Netherlands*
[3]*Institute for Theoretical Physics, Utrecht University, Leuvenlaan 4, 3584 CE Utrecht, The Netherlands*

(Received 10 November 2010; accepted 3 February 2011; published online 4 March 2011)

We present a generalized connectedness percolation theory reduced to a compact form for a large class of anisotropic particle mixtures with variable degrees of connectivity. Even though allowing for an infinite number of components, we derive a compact yet exact expression for the mean cluster size of connected particles. We apply our theory to rodlike particles taken as a model for carbon nanotubes and find that the percolation threshold is sensitive to polydispersity in length, diameter, and the level of connectivity, which may explain large variations in the experimental values for the electrical percolation threshold in carbon-nanotube composites. The calculated connectedness percolation threshold depends only on a few moments of the full distribution function. If the distribution function factorizes, then the percolation threshold is raised by the presence of thicker rods, whereas it is lowered by any length polydispersity relative to the one with the same average length and diameter. We show that for a given average length, a length distribution that is strongly skewed to shorter lengths produces the lowest threshold relative to the equivalent monodisperse one. However, if the lengths and diameters of the particles are linearly correlated, polydispersity *raises* the percolation threshold and more so for a more skewed distribution toward smaller lengths. The effect of connectivity polydispersity is studied by considering nonadditive mixtures of conductive and insulating particles, and we present tentative predictions for the percolation threshold of graphene sheets modeled as perfectly rigid, disklike particles. © *2011 American Institute of Physics*. [doi:10.1063/1.3559004]

I. INTRODUCTION

Since their discovery in the early 1990s carbon nanotubes (CNTs) have attracted a lot of attention on account of their excellent mechanical, electrical, and thermal properties. More recently, the arguably even more remarkable characteristics of another carbon allotrope, graphene sheets, were discovered.[1] Both these allotropes manifest their properties on a macroscopic level in composites involving, e.g., polymeric materials through the networks that they form in these media. It is not surprising, then, that the network formation of these nanofillers has also attracted much attention.[2,3] Indeed, a crucial requirement for obtaining the desired properties of the final composite material is controlling network formation. Provided their level of connectivity meets the criteria set by the physical property of interest, and provided they form a system-spanning network, the nanofillers can considerably improve the physical properties of the host material.[4] For example, in order to enable charge-carrier hopping or tunneling from a particle to a neighboring one in the network, they ought to be sufficiently close to each other. This required proximity sets a connectedness criterion, which in turn determines the so-called percolation threshold (PT), i.e., the minimal loading of nanofillers needed to form a domain-spanning network.[4] At this critical point, the electrical conductivity increases by many orders of magnitude.[2,3]

A considerable research effort has been devoted in determining the PT of anisometric nanofillers in composites and values as small as or smaller than 10^{-3}, measured in terms of the volume fraction that they occupy, have been found for both CNTs (Ref. 5) and graphene.[3] Such small values are not entirely surprising because both for rodlike and platelike particles the PT has been predicted to scale inversely with their aspect ratio that typically is on the order of 1000.[6–11] Indeed, graphene, being a single layer of graphite, has a typical thickness of a few angstroms and a diameter on the order of 1 μm. For the rodlike CNTs the diameters range from about 1 nm for single-walled carbon nanotubes (SWCNTs) to tens of nanometers for multiwalled carbon nanotubes (MWCNTs), whereas their lengths are generally on the micrometer scale.

In practice, preparations of nanofillers, including those of the mentioned carbon allotropes, exhibit a number of characteristics that potentially affect network formation in the preparatory stages of the composite material and hence the PT. These include a size polydispersity and the presence of nonconducting species.[3,5,12,13] In this work we focus attention on these two issues from a theoretical point of view, where we note that both CNTs and graphene sheets in the final composite normally show a large distribution in their linear dimensions. One reason for this size polydispersity is that because of strong van der Waals forces they tend to form bundles or stacks that, even after processing, are difficult to separate.[5] Because percolation phenomena are intimately related to phase transitions, which are known to be strongly influenced by polydispersity effects,[14] we expect a significant impact of polydispersity on the PT. As we show in this paper this turns out to be the case. Whether or not there is a

[a]Electronic mail: r.h.j.otten@tue.nl.

 © 2011 American Institute of Physics

Downloaded 22 Mar 2011 to 131.155.110.244. Redistribution subject to AIP license or copyright; see http://jcp.aip.org/about/rights_and_permissions

correlation between the diameters and lengths of the nanofillers we find to be a crucial question in this context, and our main claim is that the aforementioned inverse aspect ratio scaling is only true if the linear dimensions are independent of each other. A coupling between them leads to completely different behavior.

The other issue we focus on is nonadditivity. Nonadditivity of interactions has been shown to have a strong effect on the phase behavior of hard-rod dispersions[15] and hence could also be important here. As an example, we consider nonadditivity of charge transport between different kinds of particle, which implies that the connectivity range of two unlike particles differs from the average of those between pairs of like particles. In particular, we focus on the presence of nonconductive species and again expect a significant impact on the PT because, in practice, only one-third of the SWCNTs are metallic and two thirds are semiconducting.[16] This expectation turns out to be correct because we find a PT that depends very sensitively on the connectivity ranges.

The combined effects of size and connectivity variations in our view explain, at least in part, the variation of several orders of magnitude observed in PTs of CNTs that have approximately the same mean aspect ratio.[17] Theoretically, neither the effect of polydispersity in size nor that of conductivity of the nanofillers is well understood for either allotrope and often ignored in computer simulations and model predictions. For graphene, and flat particles in general, there is only a limited number of theoretical works devoted to their percolation behavior for reasons that will become apparent below. For rodlike particles, there are indeed numerous predictions but most approaches, including the reference interaction site model,[11] excluded or contact-value theorems,[6–10] and preaverage angular correlations or neglect long-range correlations.[11,18] In this paper we show that these correlations can, in fact, be very important by taking a more fundamental approach. We demonstrate that a generalized connectedness percolation theory can be reduced to a tractable form for a large class of mixtures of anisometric particles, extending our earlier paper.[19] We make use of the multicomponent pair-connectedness Ornstein–Zernike (OZ) equation, which has an analogue in the liquid-state theory,[20] where we allow for polydispersity in all three linear dimensions and connectivity ranges of the particles. From this we obtain an explicit expression for the average cluster size, with the underlying assumption that the network is formed in the fluid stages of the nanocomposite production process.[5,21]

For definiteness, we apply our theory to harshly repulsive (nonoverlapping) rodlike carbon nanotubes, invoke a second-virial approximation, and use a generalized version of the so-called cherry-pit, or core-shell model that considers two particles to be connected if they are sufficiently close to each other.[22,23] This is reasonable because nanotubes in conducting networks do not actually touch each other in the final product and charge transport across nanotubes occurs via electron hopping between them. An advantage of the cherry-pit model is that it can straightforwardly be applied to study nonadditive mixtures of conductive and nonconductive particles. With these model ingredients we find an analytical expression for the PT from the nanofiller fraction at which the cluster size diverges. Similar to what was found previously for the geometrically much simpler case of spherical particles,[24] the PT that we obtain is a function only of higher-order moments of the full size distribution notwithstanding the presence of angular correlations between the filler particles caused by translation–rotation coupling.

Our findings may be summarized as follows.

1. The PT of CNTs only depends on a few moments of the full distribution function of sizes and connectivity ranges, meaning that the details (higher moments) of these distributions are irrelevant. The combined influence of length and width polydispersity on the percolation threshold is a highly nontrivial function of the prevalence of the various species in the mixture;
2. If we assume that all CNTs are conductive and that the length and width distributions are independent of each other, then a length distribution that is strongly skewed toward shorter lengths produces the lowest PT for a fixed mean length. This generalizes prior calculations and puts these on a much firmer theoretical footing.[12,25] Thicker CNTs, on the other hand, have the opposite effect: they raise the PT and more so than expected from the inverse aspect ratio dependence valid for monodisperse tubes;
3. If the length and width distributions are coupled, which may be the case because of a sonication step, or, e.g., the screw milling part of the production process that is often employed, then neither the length nor the aspect ratio is the determining factor for a low PT. If this correlation between the length and diameter distributions is linear, the situation is completely the opposite to that of uncorrelated lengths and breadths: polydispersity raises the PT and very strongly so for a relatively small number of long rods;
4. In mixtures of conductive and insulating CNTs, which are inherently nonadditive, the PT scales with the inverse fraction of conductive filler, implying that the concentration of conductive filler particles determines the PT and the insulating ones act, in a way, as dead mass. This is specific to rodlike particles and is caused by the predominance of linear chains of interactions in the long-range correlations between them.

In the remainder of this paper we derive in Sec. II an equation for the average cluster size of mutually connected nanofillers with arbitrary distributions of their linear dimensions. In Sec. III we choose an appropriate closure and discuss the connectivity model that we use to derive the percolation threshold for rodlike CNTs, which, even in the monodisperse limit, is a nontrivial result due to the influence of translation–rotation coupling on the long-range correlations between the particles.[12] In Sec. IV we show the effect on the PT of a tetradisperse size distribution. The effect of a size polydispersity on the PT of several more realistic size distribution functions is demonstrated in Sec. V. We next apply our model to compute the effect of the presence of nonconductive particles on the PT in Sec. VI. Finally, we draw our conclusions in Sec. VII, discuss the applicability of the second-virial approximation to fillers with a different shape, and we make tentative but surprising predictions for the PT of graphene

Downloaded 22 Mar 2011 to 131.155.110.244. Redistribution subject to AIP license or copyright; see http://jcp.aip.org/about/rights_and_permissions

sheets that we model as idealized mutually repelling ("hard") disks.

II. CLUSTER-SIZE CALCULATION

Our aim is to find the percolation threshold, i.e., the minimum packing fraction of particles necessary to make the average cluster size diverge, and we attempt to obtain it from connectedness percolation theory.[20] If n_k denotes the number of clusters consisting of k particles, the weight-average overall cluster size, $S \equiv \sum_k k^2 n_k / \sum_k k n_k$, is defined as the average number of particles in a cluster containing a randomly chosen particle.[26] Given the distribution of the cluster sizes n_k, we find that the total number of contacts between two particles within the same cluster, defined as the number of pairs of particle that have a direct or an indirect connection within the same cluster, is given by $N_c = \sum_k \binom{k}{2} n_k = \frac{1}{2}\sum_k k(k-1)n_k$, with $N = \sum_k k n_k$ being the total number of particles. Hence, we deduce that $S = \sum_k (k n_k + k(k-1)n_k)/N = 1 + 2N_c/N$, which is an exact result. The first term, unity, stems from choosing a particle and the second, $2N_c/N$, from counting the particles it is in contact with in the same cluster.

The number of contacts, N_c, and the weight-average cluster size, S, can also be described in terms of the so-called pair connectedness function P. For simplicity we consider spherical particles of equal size; the generalization to polydisperse, anisometric particles is discussed below. P is defined such that $\rho^2 P(\mathbf{r}, \mathbf{r}')d\mathbf{r}d\mathbf{r}'$ is the probability of simultaneously finding a particle in a volume element $d\mathbf{r}$ at position $\mathbf{r}$ and a second particle in $d\mathbf{r}'$ at $\mathbf{r}'$, given that they are part of the same cluster.[20] Here, ρ is the number density of the particles that we presume to be uniformly distributed. This definition of P implies that $N_c = \frac{1}{2}\rho^2 \int\int d\mathbf{r}d\mathbf{r}' P(\mathbf{r}, \mathbf{r}')$ must be the total number of pairs of particle that are in contact (either directly or indirectly) in a cluster, where the factor $1/2$ corrects for double counting. If we use the property of the translational invariance of P we can write $N_c = \frac{1}{2}\rho N \int d\mathbf{r} P(\mathbf{r}, \mathbf{r}')$, which hence gives for the cluster size,

$$S = 1 + \rho \int d\mathbf{r} P(\mathbf{r}, \mathbf{r}') = 1 + \rho \lim_{\mathbf{q}\to 0} \hat{P}(\mathbf{q}), \tag{1}$$

where the hat $(.\hat{}.) \equiv \int d\mathbf{r}(\ldots)\exp(i\mathbf{q}\cdot\mathbf{r})$ denotes a spatial Fourier transform with $\mathbf{q}$ being the wave vector.

The probability $P(\mathbf{r}, \mathbf{r}')$ can be obtained by solving the pair connectedness analogue of the Ornstein–Zernike equation,[20]

$$P(\mathbf{r}, \mathbf{r}') = C^+(\mathbf{r}, \mathbf{r}') + \rho \int d\mathbf{r}'' C^+(\mathbf{r}, \mathbf{r}'') P(\mathbf{r}'', \mathbf{r}'). \tag{2}$$

Here, C^+ denotes the direct pair connectedness function that, in essence, measures short-range correlations, discussed more extensively below. An intuitive interpretation of Eq. (2) may be given as follows. The functions $P(\mathbf{r}, \mathbf{r}')$ and $C^+(\mathbf{r}, \mathbf{r}')$ describe different kinds of cluster[27] in which two particles at $\mathbf{r}$ and $\mathbf{r}'$ are connected, and Eq. (2) states that all clusters in the fluid described by the probability $P(\mathbf{r}, \mathbf{r}')$ can be subdivided into the sum of clusters with probability $C^+(\mathbf{r}, \mathbf{r}')$ that do not have any bottleneck particles that upon removal splits the cluster into two disconnected ones, and those clusters that do contain such particles.[20] Clusters from this latter type can then be divided into those that connect the first particle at $\mathbf{r}$ to the closest bottleneck particle at $\mathbf{r}''$ and another that connects $\mathbf{r}''$ to the second particle at $\mathbf{r}'$, giving $C^+(\mathbf{r}, \mathbf{r}'')P(\mathbf{r}'', \mathbf{r}')$. Averaging over all possible positions of $\mathbf{r}''$ then gives the second term in the right-hand-side of Eq. (2).

The description can straightforwardly be generalized to polydisperse, anisometric particles for which P and C^+ also depend on their linear dimensions and orientations. To describe these particles with arbitrary linear dimensions, let $x_{i\alpha\dagger}$ denote the mole fraction of particles of length L_i, width D_α, and height $H_\dagger$. In the following, we use indices with Roman symbols to denote length polydispersity, greek ones for variations in width, and the symbols †, ‡, and § to indicate different heights. The weight-average cluster size S is now the sum over the indices of the weight-average "partial cluster sizes" $S_{ij\alpha\beta\dagger\ddagger}$ that contain averages over the orientations

$$S_{ij\alpha\beta\dagger\ddagger} = x_{i\alpha\dagger}\delta_{ij}\delta_{\alpha\beta}\delta_{\dagger\ddagger} + \lim_{\mathbf{q}\to 0} x_{i\alpha\dagger}x_{j\beta\ddagger}\rho\langle \hat{P}_{ij\alpha\beta\dagger\ddagger}(\mathbf{q}, \mathbf{u}, \mathbf{u}')d\mathbf{u}d\mathbf{u}'\rangle_{\mathbf{u},\mathbf{u}'}. \tag{3}$$

Here, δ_{ij} is the Kronecker delta and $\mathbf{u} \equiv (\mathbf{u}_1, \mathbf{u}_2)$ with $\mathbf{u}_1$ and $\mathbf{u}_2$ being the unit vectors in the direction of the main axes of a particle. For the sake of notational convenience we introduced the notation $\langle\ldots\rangle_{\mathbf{u}_n} \equiv (4\pi)^{-1}\int d\mathbf{u}_n(\ldots)$, $n = 1, 2$, to denote the orientational average, with a similar prescription for the primed variables. The short-hand notation $\langle\ldots\rangle_{\mathbf{u},\mathbf{u}'}$ implies the compound average $\langle\langle\ldots\rangle_{\mathbf{u}}\rangle_{\mathbf{u}'}$. The first term of Eq. (3) is only nonzero for the particle chosen to start counting the contacts, i.e., $i = j$, $\alpha = \beta$, and $\dagger = \ddagger$, or for two different particles of equal dimensions, because for those $S_{ij\alpha\beta\dagger\ddagger}$ is the same. The second term gives the number of intracluster contacts between a particle of dimensions L_i, D_α, and $H_\dagger$ and one of dimensions L_j, D_β, and $H_\ddagger$, weighted by their mole fractions to give the correct sum.

The probability $\hat{P}_{ij\alpha\beta\dagger\ddagger}$ obeys the multicomponent analog of the pair connectedness Ornstein–Zernike equation, Eq. (2), and its Fourier transform reads

$$\hat{P}_{ij\alpha\beta\dagger\ddagger}(\mathbf{q}, \mathbf{u}, \mathbf{u}') = \hat{C}^+_{ij\alpha\beta\dagger\ddagger}(\mathbf{q}, \mathbf{u}, \mathbf{u}') + \rho\sum_{k,\gamma,\S} x_{k\gamma\S}\langle \hat{C}^+_{ik\alpha\gamma\dagger\S}(\mathbf{q}, \mathbf{u}, \mathbf{u}'') \times \hat{P}_{kj\gamma\beta\S\ddagger}(\mathbf{q}, \mathbf{u}'', \mathbf{u}')\rangle_{\mathbf{u}''}. \tag{4}$$

Because the cluster size obeys $S \equiv \sum_p S_p$ with $p \equiv \{i, j, \alpha, \beta, \dagger, \ddagger\}$, we see from Eqs. (3) and (4) that we need not solve the individual components of $\hat{P}$ but have to obtain information only on a weighted average of $\hat{P}$ over its six indices and four orientations. Therefore, detailed knowledge of the individual components of $\hat{P}_{ij\alpha\beta\dagger\ddagger}$ is not required to calculate the cluster size and the trick to solving Eq. (4) is to take averages over j, β, ‡, and $\mathbf{u}'$. For this purpose we now introduce the generalized notation $\langle\ldots\rangle_{j\beta\ddagger,\mathbf{u}} \equiv (4\pi)^{-1}\int d\mathbf{u}'\sum_{j,\beta,\ddagger} x_{j\beta\ddagger}(\ldots)$ for an average over the size distribution and the orientations of a single particle. We next

Downloaded 22 Mar 2011 to 131.155.110.244. Redistribution subject to AIP license or copyright; see http://jcp.aip.org/about/rights_and_permissions

define the functions $\Pi_{i\alpha\dagger}$ and $\Gamma_{i\alpha\dagger}$ and the operator $O_{i\alpha\dagger}$ as

$$\Pi_{i\alpha\dagger}(\mathbf{q},\mathbf{u}) \equiv \langle \hat{P}_{ij\alpha\beta\dagger\ddagger}(\mathbf{q},\mathbf{u},\mathbf{u}')\rangle_{j\beta\ddagger,\mathbf{u}'}, \tag{5}$$

$$\Gamma_{i\alpha\dagger}(\mathbf{q},\mathbf{u}) \equiv \langle \hat{C}^{+}_{ij\alpha\beta\dagger\ddagger}(\mathbf{q},\mathbf{u},\mathbf{u}')\rangle_{j\beta\ddagger,\mathbf{u}'}, \tag{6}$$

$$O_{i\alpha\dagger} f_{k\gamma\S} \equiv \rho\langle \hat{C}^{+}_{ik\alpha\gamma\dagger\S}(\mathbf{q},\mathbf{u},\mathbf{u}'') f_{k\gamma\S}(\mathbf{q},\mathbf{u}'')\rangle_{k\gamma\S,\mathbf{u}''}, \tag{7}$$

where $f_{k\gamma\S}$ is an arbitrary integrable function. This allows us to rewrite the averaged version of the OZ-equation (4) into a more compact form as

$$\Pi_{i\alpha\dagger}(\mathbf{q},\mathbf{u}) = (I_{k\gamma\S} - O_{k\gamma\S})^{-1}\Gamma_{k\gamma\S}(\mathbf{q},\mathbf{u}), \tag{8}$$

with $I_{i\alpha\dagger}$ being an operator that changes the indices of a function, so $I_{i\alpha\dagger} f_{k\gamma\S} = \sum_{k,\gamma,\S} \delta_{ik}\delta_{\alpha\gamma}\delta_{\dagger\S} f_{k\gamma\S} = f_{i\alpha\dagger}$.

According to Eq. (3), this gives for the overall average cluster size

$$S = 1 + \lim_{\mathbf{q}\to 0} \rho\langle \Pi_{i\alpha\dagger}(\mathbf{q},\mathbf{u})\rangle_{i\alpha\dagger,\mathbf{u}}. \tag{9}$$

We insert Eq. (8) into Eq. (9) for the cluster size S, note that $\Gamma_{k\gamma\S}(\mathbf{q},\mathbf{u}) = \rho^{-1} O_{k\gamma\S} 1$, and invoke the identity $1 + (I_{k\gamma\S} - O_{k\gamma\S})^{-1} O_{k\gamma\S} 1 = (I_{k\gamma\S} - O_{k\gamma\S})^{-1} I_{k\gamma\S} 1 = (I^{-1}_{k\gamma\S} (I_{k\gamma\S} - O_{k\gamma\S}))^{-1} 1$. This gives $S = \langle (I - O_{i\alpha\dagger})^{-1} 1\rangle_{i\alpha\dagger,\mathbf{u}}$, with I being the identity operator. To solve for S, we write

$$S = \langle T_{k\gamma\S}(\mathbf{u})\rangle_{k\gamma\S,\mathbf{u}}, \tag{10}$$

where T must be solved from the following simplified integral equation:

$$T_{k\gamma\S}(\mathbf{u}) - \rho\langle \hat{C}^{+}_{km\gamma\delta\S\dagger}(0,\mathbf{u},\mathbf{u}') T_{m\delta\dagger}(\mathbf{u}')\rangle_{m\delta\dagger,\mathbf{u}'} = 1. \tag{11}$$

Equations (10) and (11), which represent the central result of our theory, involve averages over the indices and orientation of a single particle as opposed to those of two particles in the original OZ-equation (4), and it follows that finding certain averages of T over its indices and argument suffices to compute the cluster size. This simplifies the calculation significantly. In Sec. III we apply our theory, valid for particles of arbitrary linear dimensions, to the rodlike carbon nanotubes. For this we invoke an appropriate closure because the direct pair connectedness function $\hat{C}^{+}$ is an as yet unknown quantity.

III. APPLICATION TO CARBON NANOTUBES

We now apply our model to carbon nanotubes, which we assume to have prefect cylindrical symmetry, so only two dimensions and a single orientation are required to describe their properties. CNTs have a typical aspect ratio of 10^2 to 10^4, and for such slender particles an accurate closure of Eq. (11) for the average cluster size is provided by the second-virial approximation.[28] See also Appendix A. This means that we consider only linear pair correlations between the particles, i.e., no loop correlations, which, as is shown below, has a significant consequence for nonadditive mixtures. The accuracy of the second-virial approximation and the possible applicability to other types of particle are considered in the discussion in Sec. VII. We first elaborate on this approximation and the connectivity model that we use and compute the percolation threshold using this approximation. To show the strong effect of polydispersity, we apply the result to a tetradisperse distribution in Sec. IV. The results are finally applied to several realistic size distributions in Sec. V, including nonadditive mixtures, in Sec. VI.

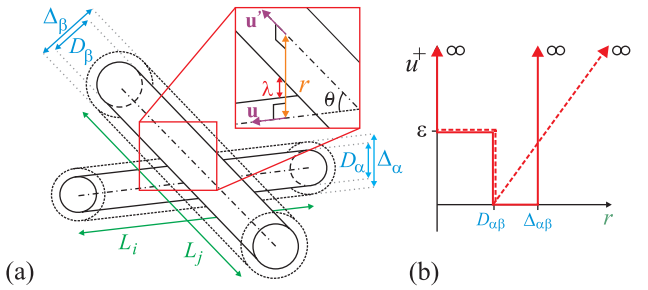

FIG. 1. (a) Schematic representation of two nanotubes with orientations $\mathbf{u}$ and $\mathbf{u}'$, lengths L_i and L_j, and diameters D_α and D_β, separated by a distance r between their centerlines and skewed at an angle θ. Charge transport between the rods requires r to be smaller than $D + \lambda = \Delta$: the dashed cylinders of diameter Δ enclosing the rods must overlap. (b) Solid line: the connectedness potential u^+ for the idealized "cherry-pit" model between two particles in the same cluster versus their distance r for ideal ($\varepsilon = 0$) and hard particles ($\varepsilon \to \infty$). The dashed line shows an alternative connectedness potential $\beta u^+ = (r - D)/\lambda$ for $r > D$ that may provide a more realistic description of an exponentially decaying electron-tunneling probability with a decay length λ. Within the second-virial approximation described in the main text, both connectedness potentials produce identical results.

The second-virial approximation implies that $\hat{C}^{+} = \hat{f}^{+}$,[9,20] with $f^{+} = \exp(-\beta u^{+})$ being the connectedness Mayer function of particles that belong to the same cluster and interact via connectedness potential u^{+}. Here, $\beta^{-1} = k_B T$, with k_B being Boltzmann's constant and T being the absolute temperature. For any configuration where two rods are not connected, this two-body connectedness potential u^{+} by definition is infinitely large. The potential that we use interpolates between ideal, penetrable particles, and hard ones that interact via a strongly repulsive excluded-volume interaction, but our final purpose is to model particles of the latter type, see Fig. 1. For intersecting particles, for which the distance r between them satisfies $r \le D_{\alpha\beta}$, we have $u^{+} = \varepsilon$, where $\varepsilon \to \infty$ for impenetrable rods and $\varepsilon = 0$ for ideal (penetrable) ones and where $D_{\alpha\beta} \equiv \frac{1}{2}(D_\alpha + D_\beta)$ denotes their average diameter. In the overlap or connectedness zone, $u^{+} = 0$ for $D_{\alpha\beta} \le r \le \Delta_{\alpha\beta}$ and $u^{+} \to \infty$ for $r \ge \Delta_{\alpha\beta}$ away from it. The length $\Delta_{\alpha\beta}$ is an adjustable parameter in our model and indicates the maximal range for effective charge transport.[12] This means that beyond this range charge transport is neglected and below we discuss the effect of a hopping probability with a longer range. The concept of the connectedness criterion is corroborated by the experimental observation that in practice the nanotubes in conducting networks do not actually touch each other;[5] our model is therefore a generalization of the so-called cherry-pit model that has earlier been used for spherical particles.[23,29]

The next step is to compute $\hat{f}^{+}$, for which it is convenient to make use of Straley's oblique coordinate system.[30] This means instead of Cartesian coordinates $\mathbf{r}$ we shift to one that has two axes along the orientations $\mathbf{u}$ and $\mathbf{u}'$ of two test rods and the third one along the shortest line connecting them,

$$\mathbf{r} = \xi\mathbf{u} + \eta\mathbf{u}' + \zeta\frac{\mathbf{u}\times\mathbf{u}'}{|\mathbf{u}\times\mathbf{u}'|}. \tag{12}$$

Downloaded 22 Mar 2011 to 131.155.110.244. Redistribution subject to AIP license or copyright; see http://jcp.aip.org/about/rights_and_permissions

The associated volume element is $d\mathbf{r} = |\sin\theta| d\xi d\eta d\zeta$, with $\theta(\mathbf{u}, \mathbf{u}')$ being the angle between the particles. For slender rods of lengths L_i and L_j, we find to leading order[31]

$$\hat{f}^+_{ij\alpha\beta}(0, \mathbf{u}, \mathbf{u}') = \int_{-L_i/2}^{L_i/2} d\xi \int_{-L_j/2}^{L_j/2} d\eta \left(\int_{-\Delta_{\alpha\beta}}^{\Delta_{\alpha\beta}} d\zeta - \int_{-D^{\text{eff}}_{\alpha\beta}}^{D^{\text{eff}}_{\alpha\beta}} d\zeta \right) \times |\sin\theta| = 2L_i L_j \left(\Delta_{\alpha\beta} - D^{\text{eff}}_{\alpha\beta}\right) |\sin\theta|, \quad (13)$$

where $D^{\text{eff}}_{\alpha\beta} \equiv D_{\alpha\beta}(1 - \exp(-\beta\varepsilon))$ is an effective diameter, so $D^{\text{eff}}_{\alpha\beta} = 0$ for ideal and $D^{\text{eff}}_{\alpha\beta} = D_{\alpha\beta}$ for hard rods. See also Fig. 1. This figure also shows an alternative potential $\beta u^+ = (r - D)/\lambda$ for $r > D$ that more realistically mimics an exponentially decaying electron-tunneling probability with a decay length λ.[32] If we use this potential instead of the cherry-pit potential and set $\lambda = \Delta_{\alpha\beta} - D_{\alpha\beta}$ as the characteristic tunneling distance, then this leaves our result, Eq. (13), for $\hat{f}^+$ invariant, so our cherry-pit model implicitly takes this effect into account.

We are now in a position to solve Eqs. (10) and (11) with the closure $C^+ = f^+$, where $\hat{f}^+$ is given by Eq. (13). Let us first tentatively presume additivity of charge-carrier hopping distances, so $\Delta_{\alpha\beta} = (\Delta_\alpha + \Delta_\beta)/2$. Nonadditivity effects caused, e.g., by a fraction of the particles not contributing to charge transport through the network, are extensively discussed in Sec. VI. For the case of additive hopping distances the cluster size S for our polydisperse CNTs can then be obtained by substituting $\hat{f}^+$ into Eq. (11), giving

$$T_{k\gamma}(\mathbf{u}) - \rho L_k \left(\Delta_\gamma - D^{\text{eff}}_\gamma\right) \langle L_m | \sin\theta | T_{m\delta}(\mathbf{u}') \rangle_{m\delta,\mathbf{u}'} - \rho L_k \left\langle L_m \left(\Delta_\delta - D^{\text{eff}}_\delta\right) | \sin\theta | T_{m\delta}(\mathbf{u}') \right\rangle_{m\delta,\mathbf{u}'} = 1, \quad (14)$$

where we have inserted within the second-virial approximation $\hat{C}^+ = \hat{f}^+$ and Eq. (13) for $\hat{f}^+$, which tacitly presumes the additivity of the overlap distance $\Delta_{\alpha\beta}$. If we average the above integral equation over $\mathbf{u}$ and use that $\langle |\sin\theta| \rangle_{\mathbf{u}} = \langle \langle |\sin\theta| \rangle_{\mathbf{u}} \rangle_{\mathbf{u}'} = \pi/4$ for an isotropic distribution of the orientations,[31] then subsequent averaging the resulting equation over the variables k and γ produces an expression for $S = \langle T_{k\gamma}(\mathbf{u}) \rangle_{k\gamma,\mathbf{u}}$ and two of its higher moments,

$$\langle T_{k\gamma}(\mathbf{u}) \rangle_{k\gamma,\mathbf{u}} - \rho \frac{\pi}{4} \left\langle L_k \left(\Delta_\gamma - D^{\text{eff}}_\gamma\right) \right\rangle_{k\gamma} \langle L_m T_{m\delta}(\mathbf{u}') \rangle_{m\delta,\mathbf{u}'} - \rho \frac{\pi}{4} \langle L_k \rangle_k \left\langle L_m \left(\Delta_\delta - D^{\text{eff}}_\delta\right) T_{m\delta}(\mathbf{u}') \right\rangle_{m\delta,\mathbf{u}'} = 1. \quad (15)$$

To solve for S, we repeat this exercise after multiplying the integral equation by L_k and $(\Delta_\gamma - D^{\text{eff}}_\gamma) L_k$, respectively.

The solution of the set of three equations that we thus obtain gives an expression for S that diverges at the PT if the rod volume fraction $\phi_p = \frac{\pi}{4} \rho \langle L_k D^2_\gamma \rangle_{k\gamma}$ obeys

$$\phi_p = \frac{\langle L_k D^2_\gamma \rangle_{k\gamma}}{\langle L^2_k \lambda^{\text{eff}}_\gamma \rangle_{k\gamma} + \sqrt{\langle L^2_k \rangle_k \langle L^2_k (\lambda^{\text{eff}}_\gamma)^2 \rangle_{k\gamma}}}, \quad (16)$$

with $\lambda^{\text{eff}}_\gamma \equiv \Delta_\gamma - D^{\text{eff}}_\gamma$. Equation (16) is our main result for dispersions of rodlike particles. We find that the PT depends only on several higher-order moments of the full distribution function. A similar result was found for spherical particles, although these obviously do not exhibit angular correlations.[24] That these are important for rods is straightforward to illustrate by means of a so-called contact-volume argument.[7] This implies that we presume that percolation requires that there is about one rod per average contact or overlap volume, which is equal to $\langle L^2_k \lambda^{\text{eff}}_\gamma \rangle_{k\gamma} \pi/2$. We then retrieve Eq. (16) except for the second term in the denominator that now becomes equal to the first term, so $\langle L^2_k \lambda^{\text{eff}}_\gamma \rangle_{k\gamma}$. The neglect of translation–rotation coupling between the rods in the "simple" contact-volume argument causes the discrepancy between the two results.

Equation (16) holds for arbitrary length and diameter distributions that are even allowed to be coupled, in which case $\langle L_k D^2_\gamma \rangle_{k\gamma} \neq \langle L_k \rangle_k \langle D^2_\gamma \rangle_\gamma$. We shall see later that a positive correlation between the distributions leads to interesting results, but we first presume the distributions to be independent. In that case ϕ_p is inversely proportional to the *weight* average $\langle L \rangle_w \equiv \langle L^2_k \rangle_k / \langle L_k \rangle_k$ of the distribution of rod lengths. A direct consequence is that a monodisperse system with only very long rods produces the lowest PT, that is, the lowest absolute value. However, the fact that the PT scales inversely with $\langle L \rangle_w$, not the number average $\langle L_k \rangle_k$, causes cooperative behavior between the rods that has a significant impact on the PT. Indeed, the dependence on the weight average implies that increasing the length polydispersity lowers the PT for a constant average length because longer rods contribute more to the growing network than shorter ones do, and the effect is stronger for a larger length difference.

In Secs. IV– VI, the results from this section are applied to systems that can be considered as implementations of our model. The first application in Sec. IV is an idealized system of tetradisperse rods that shows a sensitive dependence of the PT on a size polydispersity. Next, in Sec. V we consider more realistic distributions to demonstrate that a large decrease in the PT requires a length distribution that is strongly skewed toward shorter lengths. The final application of our model is in Sec. VI, where we find a sensitive dependence of the PT on the presence of nonconductive particles in the distribution.

IV. TETRADISPERSE DISTRIBUTION

We first apply our main result for rodlike particles, Eq. (16), to a tetradisperse system system of long, short, thick, and thin rods, where the thick rods model either MWCNTs or bundles of CNTs. This distribution has a very strong effect on the PT, as is illustrated in Fig. 2. We see that the PT increases linearly with the mole fraction of thick rods, whereas it decreases with the fraction of long rods. The larger the length difference, the smaller the fraction of long rods required to realize a significant reduction in the PT. For a length ratio of more than 8 the PT is decreased by a factor of more than 4 by adding only 10% of long rods, and it is reduced further only slightly by adding long ones. We note that here the distributions are presumed to be independent of each other, which turns out to be an important assumption to be discussed in Sec. V.

The reciprocal weight-average length dependence of the PT that we find agrees with results for interpenetrable sticks[7] and hard rods with monodisperse diameters and connectivity ranges,[12] for which we find $\phi_p = D^2/2\langle L \rangle_w \lambda$, with $\lambda = \Delta$

Downloaded 22 Mar 2011 to 131.155.110.244. Redistribution subject to AIP license or copyright; see http://jcp.aip.org/about/rights_and_permissions

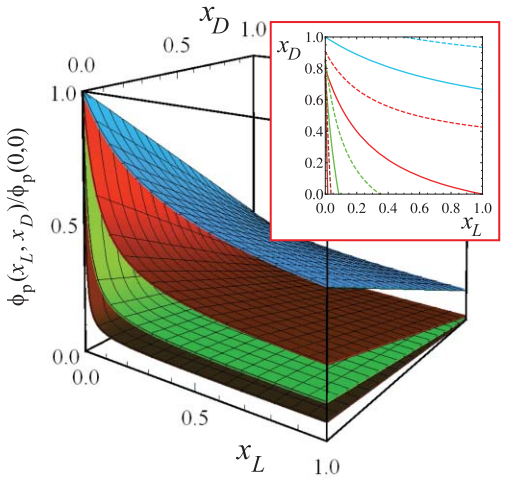

FIG. 2. For a tetradisperse mixture of thick, thin, long, and short rods the percolation threshold ϕ_p is shown as a function of the number fractions x_L of long rods and x_D of thin rods. The tunneling length λ is taken as a constant and drops out of the description. The graphs are for different length ratios ($n \equiv L_{\text{long}}/L_{\text{short}}$) and width ratios ($D_{\text{thick}}/D_{\text{thin}}$), which are taken equal to n. From top to bottom: $n = 2, 4, 8$, and 16. Inset: the nonlinear behavior of ϕ_p is demonstrated by a cross section for constant $\phi_p(x_L, x_D)/\phi_p(0,0) = 0.25$ (0.15) for the solid (dashed) lines. Pairs of line from top right to bottom left: $n = 2, 4, 8$, and 16.

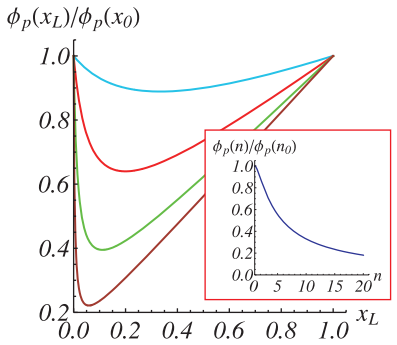

FIG. 3. For a bidisperse mixture of long and short rods the ratio of the actual percolation threshold $\phi_p(x_L)$ and that of the corresponding monodisperse solution $\phi_p(x_0)$ with the same mean length $\langle L_k \rangle_k$ is shown as a function of the number fraction x_L of long rods. The tunneling length λ is taken as a constant and in that case drops out of this ratio. The graphs are for different length ratios $n \equiv L_{\text{long}}/L_{\text{short}}$ and we find $x_0 = nx/(1 + (n-1)x)$. From top to bottom, $n = 2, 4, 8$, and 16. Inset: the largest reduction of the ratio of PTs is $\phi_p(n)/\phi_p(n_0) = 4n/(n+1)^2$, with $n_0 = (3n-1)/(n+1)$, obtained for $x = 1/(n+1)$, i.e., the minima in the main graph.

$-D$. The value of λ plausibly depends on the dielectric constant of the host medium[12] and can also effectively be manipulated by a penetrable conductive coating of the CNTs, such as the conductive polymer blend poly(3,4-ethylenedioxythiophene):poly(styrene sulfonate) (PEDOT:PSS),[21,33] discussed in more detail in Sec. VI. In the monodisperse limit we find $\phi_p = D^2/2\lambda L$ for hard particles, in agreement with recent analytical work.[32] For ideal particles in the same limit we find $\phi_p = D^2/2\Delta L = D/2L$ with $D_\gamma^{\text{eff}} = 0$, where we put $\Delta = D$.[12] This is also consistent with computer simulations[34] and with results that were based on geometric arguments.[9,25,35]

In order to highlight the strong cooperative behavior between the rods for small fractions of long ones and to make the highly nonlinear effect of polydispersity more quantitative, we calculate Eq. (16) and compare this with that for the monodisperse case for which $\langle L_i^a D_\alpha^b \rangle_{i\alpha} = L^a D^b$ for the integers powers $a, b = 0, 1, 2 \ldots$. We consider polydisperse distributions that obey $\langle L_i \rangle_i^a \langle D_\alpha \rangle_\alpha^b = L^a D^b$, so they have the same *number* averages as the reference monodisperse case. It appears reasonable to presume the hopping distance λ to be an invariant of the dimensions of the CNTs, so we divide Eq. (16) by $\langle D_\alpha \rangle_\alpha^2 / 2\lambda \langle L_i \rangle_i$ and obtain for the ratio of percolation thresholds $\phi_p(x, y)/\phi_p(x_0, y_0) = \langle L_i \rangle_i^2 \langle D_\alpha^2 \rangle_\alpha / \langle L_i^2 \rangle_i \langle D_\alpha \rangle_\alpha^2$. Here, x and y are as yet unspecified parameters that depend on the type of length and diameter distributions adopted and that measure the degree of polydispersity; x_0 and y_0 are the values for which the distribution is monodisperse, i.e., very strongly peaked, with the same number average.

We observe that the polydispersity indices $\langle L_i^2 \rangle_i / \langle L_i \rangle_i^2$ and $\langle D_\alpha^2 \rangle_\alpha / \langle D_\alpha \rangle_\alpha^2$ of the distributions suffice to determine the effect of polydispersity on the PT. If we insert the identities $\langle D_\alpha^2 \rangle_\alpha = \text{Var}(D_\alpha) + \langle D_\alpha \rangle_\alpha^2$ and $\langle L_i \rangle_i^2 = \text{Var}(L_i) + \langle L_i \rangle_i^2$, where Var denotes the variance of a distribution, we obtain

$$\frac{\phi_p(x, y)}{\phi_p(x_0, y_0)} = \frac{m+1}{s+1}, \tag{17}$$

with $m \equiv \text{Var}(D_\alpha)/\langle D_\alpha \rangle_\alpha^2$ and $s \equiv \text{Var}(L_i)/\langle L_i \rangle_i^2$ being the relative magnitudes of the variances of the diameter and length distributions.[36] Equation (17) shows that a small value of m and large value of s are required for a significant reduction of the PT relative to the equivalent monodisperse distribution. Given that m is positive for any distribution that is not monodisperse, width polydispersity apparently raises the PT. However, in practice m remains close to unity because for both SWCNTs and MWCNTs, we estimate it to be at most 0.2.[37,38] As to the influence of a length polydispersity, the fact that a large value of s leads to a low PT is an important issue that we return to in the discussion.

If we consider a bidisperse mixture consisting of long and short rods, we find that $x_0 = nx/(1 + (n-1)x)$, and we observe that a large value of s is obtained for a large skewness of the distribution, that is, a skewness toward smaller lengths, as is illustrated in Fig. 3. Indeed, by adding a small fraction of long rods to a dispersion of short ones that are n times shorter, a significant nonlinear reduction can be obtained. This additional reduction decreases again with increasing fraction of long rods, where we note that the absolute minimal PT is course obtained if all rods are long. The maximal reduction of the PT relative to the equivalent monodisperse system is reached for a number fraction x_L of long ones that satisfies $x_L = 1/(n+1)$, so the larger the length difference, the smaller the fraction of long rods required to realize a significant reduction of the PT. At this optimum number fraction the relative PT equals $\phi_p(n)/\phi_p(n_0) = 4n/(n+1)^2$, where, $n_0 = (3n-1)/(n+1)$, see also Fig. 3. So, a mixture containing only 11% of rods that are eight times longer has a PT that is more than 60% lower than the monodisperse system with the same average length. This finding may then provide an explanation for the large scatter in observed PTs of

Downloaded 22 Mar 2011 to 131.155.110.244. Redistribution subject to AIP license or copyright; see http://jcp.aip.org/about/rights_and_permissions

CNTs with the same (number) average dimensions.[17] A more generalized analysis that we present in Sec. V and discuss in Sec. VII teaches us that a length distribution that is strongly skewed toward shorter lengths, as shown in Fig. 3, is in fact a *requirement* for a large reduction of the PT. In Sec. V we will also consider the impact of polydispersity on the PT of other length and width distributions inspired by experimental observations.

V. REALISTIC SIZE DISTRIBUTIONS

Let us now turn to perhaps somewhat more realistic size distributions of CNTs than the tetravalent one discussed in Sec. IV, and for these we compute the effect that they have on the percolation threshold. Because of a lack of experimental data, we first consider independent length and width distributions; coupled distributions are discussed further on in this section. We showed in Sec. IV that a width polydispersity in practice raises the PT only marginally, so we take constant CNT diameters and we focus on length polydispersity. Based on the very few available experimental measurements of the length distribution of CNTs, we choose a Gamma distribution and the related Weibull distribution.[39–42] A limiting case of both of these distributions is the exponential distribution with a probability density function (PDF) $f_e(L) = \eta \exp(-\eta L)$,[43,44] for which $\phi_p(\eta)/\phi_p(\eta_0) = 1/2$, with $\eta_0 = \eta/2$, irrespective of the value of the distribution parameter η that takes the form of the inverse mean length.[45] So, an exponential distribution reduces the PT by a factor of 2 (relative to the equivalent monodisperse case). Parenthetically, we note that the exponential distribution is characterized by a single independent moment only.

The Gamma distribution is described by *two* independent moments and obeys a PDF of the form $f_\Gamma(L) = L^{k-1} \exp(-L/\theta)\theta^{-k}/\Gamma(k)$, with $\Gamma(k)$ the Gamma function.[45] Its first few moments are $\langle L_i \rangle_i = k\,\theta$, $\langle L_i^2 \rangle_i = k(k+1)\,\theta^2$, $\langle L_i^3 \rangle_i = k(k+1)(k+2)\,\theta^3$. The scale parameter θ leaves the shape invariant and only rescales the distribution; k is the shape parameter and for smaller values the spread in the distribution increases because the earlier defined scaled variance obeys $s = 1/k$. The monodisperse limit corresponds to $k \to \infty$, whereas for smaller values of k the distribution becomes more skewed toward smaller lengths. The skewness γ is usually defined as $\gamma \equiv \langle (L_i - \langle L_i \rangle_i)^3 \rangle_i / \langle (L_i - \langle L_i \rangle_i)^2 \rangle_i^{3/2}$,[45] implying that there are many more short CNTs than long ones for a large positive skewness and vice versa for a large negative one. For the Gamma distribution the skewness and shape parameter are related via $\gamma = 2/\sqrt{k} \geq 0$, which goes to zero for a large value of k. We find that $\phi_p(k)/\phi_p(\infty) = k/(k+1)$, which becomes very small for a small k, or, equivalently, a large positive skewness. The results are shown in Fig. 4. Given that we consider the distributions at equal first moment $\langle L_i \rangle_i$ and that we have only two independent moments, $\phi_p(k)/\phi_p(\infty)$ can also be expressed in terms of the relative magnitude s of the variance because $s = 1/k$ and $\gamma = 2\sqrt{s}$. This agrees with the earlier result $\phi_p(s)/\phi_p(0) = 1/(s+1)$ and shows that a large value of s is accompanied by a large skewness for this distribution.

The Weibull distribution is defined by the PDF $f_W(L) = a\,b\,L^{b-1} \exp(-aL^b)$, with $a > 0$ the scale parameter and $b > 0$ the shape parameter. The distribution has as its first moments $\langle L_i \rangle_i = \Gamma(1/b)/b\ a^{1/b}$, $\langle L_i^2 \rangle_i = \Gamma(1+2/b)/a^{2/b}$, and $\langle L_i^3 \rangle_i = \Gamma(1+3/b)/a^{3/b}$. The parameter a has no effect on the skewness γ nor on the scaled variance or spread $s = -1 + 2b\,\Gamma(2/b)/\Gamma(1/b)^2$. The skewness is a complicated expression of Gamma functions and can become negative, unlike that of the Gamma distribution. The monodisperse limit corresponds to a vanishing spread s, which occurs in the limit of $b \to \infty$, in which case γ converges to the finite value $-12\sqrt{6}\,\zeta(3)/\pi^3 \approx -1.14$,[46] with ζ being the Riemann zeta function.[47] The ratio of the PTs again only depends on the shape parameter via $\phi_p(b)/\phi_p(\infty) = \Gamma(1+1/b)^2/\Gamma(1+2/b)$. We have plotted this function in Fig. 5, and we again observe that for the polydisperse and equivalent monodisperse cases this ratio decreases for increasing skewness, which also implies an increase of the variance, just as is the case for the Gamma distribution.

In conclusion, we find from Figs. 4 and 5 that for both the Gamma and the Weibull distributions the nonlinearity in the reduction and hence also the absolute reduction of the PT can be significant and that a length polydispersity can substantially lower the PT at equal average length. For this to be the case, the distributions need to have a large positive skewness γ (larger than, say, 2), or, equivalently, a large scaled variance s. Clearly, this coupling between the skewness and the spread is not present for a distribution with more than two independent moments, but in the discussion below we show that a large value of s does actually imply a large skewness and that a large variance without any skewness is not sufficient to obtain a low PT. In any event, for those few CNT systems for which the moments of the length distributions have actually been determined, the skewness and spread seem to be quite small, i.e., $\gamma = 0.40$ and $s = 0.20$, giving $\phi_p(x)/\phi_p(x_0) = 0.84$,[40] or $\phi_p(x)/\phi_p(x_0) = 0.64$,[48] or $\phi_p(x)/\phi_p(x_0) = 0.50$ for an exponential distribution;[43,44] so for these the effect of polydispersity is modest. Given the very large scatter in measured PTs of carbon-nanotube composites,[17] we conclude that the skewness in the distributions must usually, in fact, be much larger than this. In support of this conjecture, we note that it is quite plausible that during the sonication of the CNTs, a necessary exfoliation step in the production process of the nanocomposite pushes the distribution of CNTs to become very skewed toward the direction of the shorter rods.[5,21] Indeed, exfoliation goes hand-in-hand with tube scission, and long tubes break more easily than short ones.[49] In fact, wide tubes break less easily than narrow ones, casting doubt on the assumption of independent length and width distributions that we presumed so far. This turns out to be a crucial insight. This implies that the length and diameter distributions must be positively correlated.

We saw above that in order to obtain a low PT, all rods should be thin and the length distribution must have a large positive skewness, so it must decay rapidly with the rod length. However, if the length and width distributions have a positive correlation, then the consequences of such a length distribution are completely different. To estimate the level of correlation, one could argue that the probability of breaking

Downloaded 22 Mar 2011 to 131.155.110.244. Redistribution subject to AIP license or copyright; see http://jcp.aip.org/about/rights_and_permissions

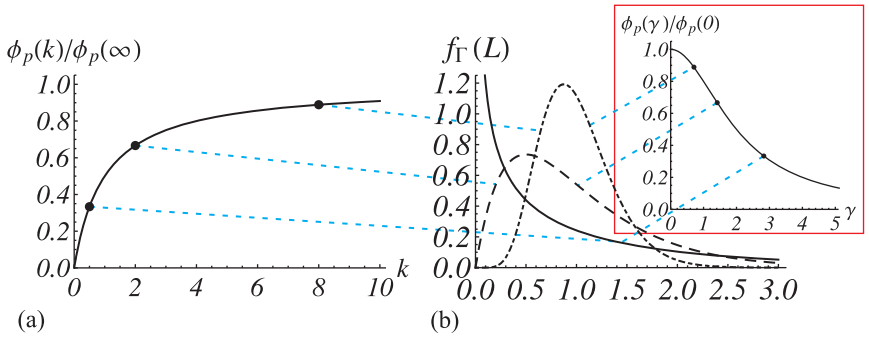

FIG. 4. (a) The influence of length polydispersity on the ratio of the PTs of the Gamma distribution and that of the corresponding monodisperse distribution with equal mean length, $\phi_p(k)/\phi_p(\infty) = k/(k+1)$. The tunneling length λ is taken as a constant and in that case drops out of the equation. The ratio of the PTs depends only on the shape parameter k, which is infinitely large for a monodisperse distribution, and the effect can be strong for small k values. (b) For the values $k = 1/2$, 2, and 8 from (a) the distributions are shown that all have the same mean $\langle L_k\rangle_k = k\,\theta = 1$ and the PT values relative to that in the monodisperse limit are $\phi_p(k)/\phi_p(\infty) = 1/3$ (solid), $2/3$ (dashed), and $8/9$ (dashed-dotted). Inset: the impact of the length polydispersity can also be expressed in terms of the skewness $\gamma = 2/\sqrt{k}$ of the distribution, showing that for a large skewness the reduction of the PT is significant. The three points marked on the graph correspond to the three distributions.

a rod in two is proportional to the required scission energy under sonication, which in turn scales with the area of the cross section of, e.g., MWCNTs at least if they are sufficiently wide. We recall that MWCNTs tend to have a broad spread in widths. But if $L_i = \alpha D_\gamma^2$, with α being a positive constant, then there would be *no* dependence of the PT on the size distributions at all because according to Eq. (16) the PT then becomes equal to $\phi_p = (2\alpha\lambda)^{-1}$, that is, if we presume the tunneling range λ to be constant. (This is by no means certain of course.)

SWCNTs also exhibit a diameter variation[39,50] and for these the scission energy, which is proportional to the number of bonds that have to be broken, presumably scales linearly with the diameter. If $D_\gamma = \alpha L_i$, we find that $\phi_p(x) = \alpha^2\langle L_i^3\rangle_i/2\lambda\langle L_i^2\rangle_i$ and $\phi_p(x_0) = \alpha^2\langle L_i\rangle_i/2\lambda$, so $\phi_p(x)/\phi_p(x_0) = \langle L_i^3\rangle_i/\langle L_i\rangle_i\langle L_i^2\rangle_i$. If we evaluate this for a Gamma, a Weibull, and an exponential distribution, we find that the competition between a desired large length and small diameter causes the PT to be *raised* by polydispersity, not decreased, so the PT is in that case always higher than that of the corresponding monodisperse distribution, see Fig. 6. The effect becomes stronger for smaller values of b and k, i.e., a larger positive skewness and lower spread in the distribution. This result is exactly the opposite of what we obtained for uncorrelated distributions. In conclusion, we find that the level of correlation between the lengths and widths of rodike particle formulations is indeed crucial for the dependence of the percolation threshold upon the polydispersity. Depending on this, polydispersity effects may either raise or lower the PT relative to that of the monodisperse case.

We next address another form of polydispersity often ignored in theoretical studies, being that in the level in which the CNTs conduct electricity.

VI. MIXTURES OF CONDUCTIVE AND INSULATING PARTICLES

In Secs. III–V we have tacitly assumed that all CNTs contribute to the percolating network and that connectivity is an additive property, i.e., $\Delta_{\alpha\beta} = (\Delta_\alpha + \Delta_\beta)/2$. If the nanocomposite contains not only conductive but also semi-conductive or insulating particles, which is certainly true for SWCNTs, then this additivity assumption breaks down because a charge carrier can only move between a pair of conductive particles and its transport is effectively blocked if one or both of

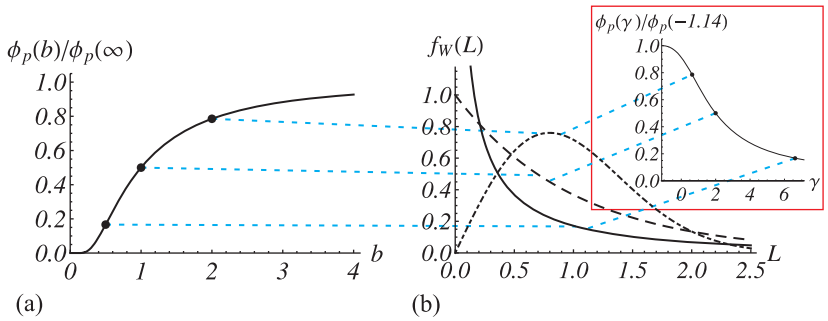

FIG. 5. (a) For a Weibull distribution the effect of length polydispersity on the ratio of the PTs of the Weibull distribution and that of the corresponding monodisperse distribution with equal mean length, $\phi_p(b)/\phi_p(\infty) = \Gamma(1+1/b)^2/\Gamma(1+2/b)$ with Γ the Gamma function (Ref. 45). The tunneling length λ is taken as a constant and in that case drops out of the equation. The ratio depends only on the shape parameter b. The scaled variance s goes to zero in the monodisperse limit that $b \to \infty$, in which case the skewness $\gamma \to -1.14$. A large reduction of the PT is observed for small b. (b) Three Weibull distributions with $\langle L_i\rangle_i = 1$ are shown for the values $b = 1/2$, 1, and 2, for which $\phi_p(k)/\phi_p(\infty) = 0.17$ (solid), 0.5 (dashed), and 0.79 (dashed-dotted). Inset: the impact of polydispersity can also be expressed in terms of the skewness γ of the distribution, showing that for a large skewness the reduction of the PT is significant. The three points marked on the graph correspond to the three distributions.

Downloaded 22 Mar 2011 to 131.155.110.244. Redistribution subject to AIP license or copyright; see http://jcp.aip.org/about/rights_and_permissions

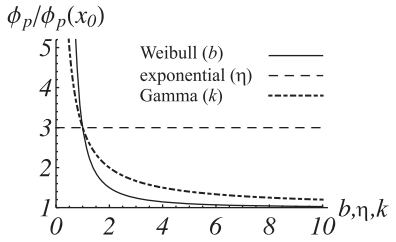

FIG. 6. The percolation threshold ϕ_p for a polydisperse distribution relative to its value $\phi_p(x_0)$ for the corresponding monodisperse case with the same mean length and diameter is shown for length and diameter distributions that are linearly correlated, i.e., $L_i = \alpha D_i$, with α being a constant. For a constant tunneling length λ, polydispersity *raises* the PT for the Weibull, Gamma, and exponential distributions, and most predominantly for small values of the shape parameter b and k of the Weibull and Gamma distributions, meaning a large skewness and large spread. For the exponential distribution the PT is raised by a factor of 3, regardless of the shape parameter η that equals the reciprocal of the mean value of the distribution.

them are poor conductors. Fortunately, our theory can quite straightforwardly be adjusted to model a mixture of metallic and electrically insulating rods, at least if they are of equal diameter. This is obviously an idealization because the single-walled CNTs that do not possess metallic properties are not perfect insulators and, as already alluded to, exhibit semiconducting behavior,[2] but for our purposes this model suffices.

In our model description we take our familiar criterion for connectivity of a pair of conductive rods, i.e., $\Delta_{11} = D + \lambda$, with the subscript 1 referring to the conductive species, and we require that particles of any other pair need to touch for charge transport to take place, which statistically occurs with zero probability. This means that $\Delta_{12} = \Delta_{22} = D$, where the subscript 2 indicates an insulating rod. This enforces nonadditive charge-transport properties by blocking charge transport if at least one of the particles in a pair is not metallic. We consider a binary mixture of conductive and insulating rods of mole fractions x and $1 - x$, respectively. We then start from Eq. (14) that we average over $\mathbf{u}$, and obtain

$$\langle T_{k\gamma}(\mathbf{u})\rangle_{\mathbf{u}} - \frac{\pi}{2}\rho L_k \langle (\Delta_{\gamma\delta} - D) L_m T_{m\delta}(\mathbf{u}')\rangle_{m\delta,\mathbf{u}'} = 1. \quad (18)$$

If the index $\gamma = 2$ refers to the insulating particles, we have $\langle(\Delta_{2\delta} - D)T_{m\delta}(\mathbf{u}')\rangle_\delta = 0$ and for $\gamma = 1$, denoting the conducting particles, we have $\langle(\Delta_{1\delta} - D)T_{m\delta}(\mathbf{u}')\rangle_\delta = \lambda\, x\, T_{m1}(\mathbf{u}')$. We substitute this in Eq. (18) and obtain $\langle T_{k1}(\mathbf{u})\rangle_{\mathbf{u}} - \frac{\pi}{2}\rho\,\lambda\, x\, L_k \langle L_m T_{m1}(\mathbf{u}')\rangle_{m,\mathbf{u}'} = 1$. We take averages over k after subsequently multiplying it by unity and by L_k. Solving the resulting set of equations for $\langle T_{k1}(\mathbf{u})\rangle_{k,\mathbf{u}}$ and $\langle L_k T_{k1}(\mathbf{u})\rangle_{k,\mathbf{u}}$ gives for the former

$$\langle T_{k1}(\mathbf{u})\rangle_{k,\mathbf{u}} = \frac{1 - \frac{\pi}{2}\rho\,\lambda\, x\, \mathrm{Var}(L_k)}{1 - \frac{\pi}{2}\rho\lambda\, x\, \langle L_k^2\rangle_k}, \quad (19)$$

which diverges if the denominator is zero, leading to the critical number density $\rho_p = (\frac{\pi}{2}\,\lambda\, x\, \langle L_k^2\rangle_k)^{-1}$. From this we find for the PT

$$\phi_p = \frac{\pi}{4}\langle L_k\rangle_k D^2 \rho_p = \frac{D^2\langle L_k\rangle_k}{2\,\lambda\, x \langle L_k^2\rangle_k}. \quad (20)$$

We see that we retrieve our previous result, Eq. (16), for polydisperse lengths but monodisperse widths, except for an additional factor $1/x$. Hence, we find that the percolation threshold is governed by the fraction $x\,\phi$ of conductive particles. This means that if one third of the SWCNTs is conductive, as is believed to be the case,[51] then the PT is three times larger than would have been if all of them had been conductive, implying that increasing the fraction of conductive CNTs is a useful endeavor if a low PT is required for the nanocomposite application envisaged.[5,51,52] The fact that the PT is governed completely by the concentration of conductive particles may seem counter intuitive, the reason being that the presence of nonconductive fillers should cause a disproportionate increase of the PT because they can take out entire conductive paths in a network that spans the whole system. We surmise that this effect is counteracted by nonconductive particles that sit in dead branches and would have no contribution to the network anyway. In fact, this prediction can be understood at a deeper level if we consider percolation on a Bethe lattice. A Bethe lattice is a cycle-free tree with z branches per lattice site, allowing us to readily deduce that provided a fraction x of these particles contributes to the charge transport, it must have a PT of $\phi_p = 1/x(z-1)$ if expressed in terms of the fraction of occupied sites.[4] From this result we conclude that the $1/x$ scaling in the PT must be the result of the absence of loop correlations in the Bethe lattice, which it has in common with the second-virial approximation in continuous space.[19]

Another way to achieve the goal of lowering the PT is to make use of an electrically conducting coating of the CNTs, replacing the surfactants that often are used to disperse the CNTs in water in the early stages of the production process of the nanocomposite.[21] This coating then in a way manipulates the (effective) hopping distance λ, provided it is in a way soft and physically penetrable to other CNTs.[53] For such a coating, a polymeric latex known as PEDOT:PSS has been used that also effectively stabilizes the CNTs in a solution.[21,33] We note that the envisaged conduction mechanism of nearest-neighbor hopping in our model may lose its meaning for the rods with the soft conductive coating. Still, if we presume that the effective hopping distance is much larger for a coated CNT than for one without a coating, then the probability of charge transport between two CNTs without a coating is negligible compared to that of a pair with at least one coated particle. This implies that $\Delta_{11} = D + \lambda$, $\Delta_{12} = D + \lambda/2$, and $\Delta_{22} = D$, where the subscript 1 (2) indicates the (non-)conductive particle. In this model conduction takes place via the intersection of two coatings or via the intersection of a coating and a rod.

If this is so, we have for the average $\langle(\Delta_{2\delta} - D)T_{m\delta}(\mathbf{u}')\rangle_\delta = \frac{\lambda}{2}\, x\, T_{m1}(\mathbf{u}')$ in Eq. (18) for the index $\gamma = 2$ and $\langle(\Delta_{1\delta} - D)T_{m\delta}(\mathbf{u}')\rangle_\delta = \lambda\, x\, T_{m1}(\mathbf{u}') + \frac{\lambda}{2}(1-x)T_{m2}(\mathbf{u}')$ for the index $\gamma = 1$, where x now stands for the mole fraction of coated CNTs. If we insert this in Eq. (18) we obtain the following set of equations:

$$\langle T_{k1}(\mathbf{u})\rangle_{\mathbf{u}} - \frac{\pi}{2}\rho L_k \Big(\lambda x \langle L_m T_{m1}(\mathbf{u}')\rangle_{m,\mathbf{u}'} + \frac{\lambda}{2}(1-x)\langle L_m T_{m2}(\mathbf{u}')\rangle_{m,\mathbf{u}'}\Big) = 1, \quad (21)$$

$$\langle T_{k2}(\mathbf{u})\rangle_{\mathbf{u}} - \frac{\pi}{4}\rho\,\lambda\, x L_k \langle L_m T_{m1}(\mathbf{u}')\rangle_{m,\mathbf{u}'} = 1, \quad (22)$$

Downloaded 22 Mar 2011 to 131.155.110.244. Redistribution subject to AIP license or copyright; see http://jcp.aip.org/about/rights_and_permissions

for the two types of particle in the dispersion. If we take the average of Eqs. (21) and (22) over k after multiplying them by unity and by L_k, we have four equations for the four unknowns $\langle T_{k1}(\mathbf{u})\rangle_{k,\mathbf{u}}$, $\langle T_{k2}(\mathbf{u})\rangle_{k,\mathbf{u}}$, $\langle L_k T_{k1}(\mathbf{u})\rangle_{k,\mathbf{u}}$, and $\langle L_k T_{k2}(\mathbf{u})\rangle_{k,\mathbf{u}}$. We solve these and find that the solutions have as a common denominator $16-\pi\lambda\rho\, x\langle L_k^2\rangle_k(8+\pi\lambda\rho\,(1-x)\langle L_k^2\rangle_k)$, which vanishes at the critical number density $\rho_p=((\sqrt{x}+x)\langle L_k^2\rangle_k\pi\lambda/4)^{-1}$. This then gives

$$\phi_p=\frac{D^2\langle L_k\rangle_k}{(\sqrt{x}+x)\lambda\langle L_k^2\rangle_k}, \tag{23}$$

for the PT. So, we find a nontrivial dependence of the PT on the fraction of coated rods x. Again, the larger the fraction of coated rods, the lower the PT, as is to be expected.

One may ask what would be the PT of PEDOT:PSS coated nanotubes that are poor conductors instead of metallic ones—an experiment recently conducted by Hermant *et al.*[21,33] In that case the particles may only serve as a scaffold that still allows the conductive material to percolate at very low loadings, so charge transport is then only possible, provided two coatings intersect. This case is equivalent to the one we discussed earlier, i.e., mixtures of the conducting and nonconducting nanotubes. Comparing Eqs. (20) and (23) we conclude that there is an additional factor $2x/(\sqrt{x}+x)$ determining the PT that can be gained by taking conductive instead of insulating rods, which is quite significant if x is not very close to unity.

Inspired by the experiments of Hermant, we can now conduct a thought experiment to demonstrate this effect. We determine the PT of high-quality (metallic) SWCNTs, and use a small amount of conductive, penetrable coating material that we presume to fully cover a small fraction of the SWCNTs. If we perform the same experiment on poor-quality (insulating) SWCNTs, then according to the above observation, the PT should be more than a factor of 2 lower if the fraction of coated CNTs is less than only 10%. Hence, there should be a considerable difference between using conductive and insulating filler particles, suggesting that for incomplete surface coverage the fillers not only serve as a scaffold.

VII. DISCUSSION AND CONCLUSIONS

In this paper we have presented a systematic approach to study the effect of size and connectivity polydispersity on connectedness percolation for a large class of particle dispersions. Using the multicomponent pair-connectedness Ornstein–Zernike equation that depends on the properties of pairs of particle, we derived an expression for the average cluster size of connected particles, requiring as input only some average of a function that depends on the properties of a *single* (test) particle. By choosing an appropriate closure for this expression, we obtained an analytical expression for the percolation threshold of the conductive rodlike particles. It turns out to be a nontrivial function of the composition of lengths, widths, and connectivity ranges, yet depends on a few moments of the full distribution. This implies that for the PT one only needs to know these moments and the details of the distribution are irrelevant.

We find that the inverse aspect ratio scaling of the PT, although often assumed, only holds if the length and width distributions are uncorrelated, which may be quite a strong assumption, considering the sonication step often used in the nanocomposite production process. If the length and width distributions are indeed uncorrelated, we deduce that the presence of wider rods raises the PT and slightly more so than based on the inverse aspect ratio dependence of it for monodisperse ones, while a length polydispersity significantly lowers the PT at equal number average for small fractions of longer rods. For a bidisperse system this latter effect is very strong, indeed, provided the length difference is large and the main component of the mixture consists of short rods. For the plausibly more realistic length distributions such as the Gamma and Weibull distributions, we also find a large decrease in the PT, again only if the distribution is strongly skewed toward shorter lengths. This may seem somewhat surprising because $\phi_p(x)/\phi_p(x_0)=1/(s+1)$, with $s\equiv \mathrm{Var}(L_k)/\langle L_k\rangle_k^2$, depends only on the ratio of the variance and the mean of the lengths of the rods.

However, it so happens that a large positive skewness γ is a necessary condition for a significant decrease of the PT and that a large variance is not sufficient to obtain a large value of the parameter s. The reason is that a standard deviation of a stochastic variable cannot be large compared to the mean value unless the distribution is strongly skewed. This we cannot prove conclusively from our results for the Gamma and Weibull distributions because these distributions have only two independent moments. For these distributions only one moment can be varied independently, and for a fixed average length a large positive skewness goes hand-in-hand with a large value of s. On the other hand, for symmetric distributions, so without any skewness, we can show that the one with the largest value of s, which is a bidisperse mixture, has a *maximum* value of $s=1$. We refer to Appendix B for details. This means that the largest decrease of the PT as a result of a symmetric length distribution is a factor of 2. From the bidisperse mixture in Fig. 3 we have seen that a considerably larger reduction of the PT can be obtained by taking a distribution that is strongly skewed toward shorter lengths and that has a large length ratio. Also, from our results for the skewed Gamma and Weibull distributions it follows that polydispersity can cause the PT to decrease much more than this factor of 2. It is for these reasons that a large positive skewness in the length distribution is a requirement for a significant decrease in the percolation threshold.

Still, for the realistic distributions with a large skewness we studied, the effect of length polydispersity appears not to be strong enough to explain the scatter of multiple orders of magnitude in observed PTs of carbon nanotubes with the same average dimensions.[17] We speculate that the few size distributions available in the literature[37–44] are not representative of the ones that have been used in the production of the percolating networks in CNT composites. Although a speculation, we feel it is plausible because sonication and, in some preparation procedures, screw extrusion[54] causes a larger skewness toward short lengths. These processing steps may have an additional and rather profound effect on the PT because the breakup of larger nanotubes into smaller ones may

Downloaded 22 Mar 2011 to 131.155.110.244. Redistribution subject to AIP license or copyright; see http://jcp.aip.org/about/rights_and_permissions

induce a positive correlation between the length and diameter distributions. This leads to a completely different situation from the one where their covariance is zero. Most importantly, we find that neither the aspect ratio nor the length of the CNTs is the determining factor for the PT, but there is a sensitive dependence on the coupling of the distribution functions and the relevant higher-order moments. A linear correlation seems plausible for SWCNTs because the probability of breaking is proportional to the scission energy, which in turn scales with the number of bonds to be broken and has a linear relation with the perimeter. In that case the effect of polydispersity is exactly the reverse of what we observe for independent distributions: polydispersity raises the PT and the effect is stronger for a larger positive skewness in the distribution. The sensitivity to the coupling is exemplified even more if we assume the length to be proportional to the square of the diameter, which seems more appropriate for MWCNTs because for those the number of bonds scales linearly with the area of the cross section. This correlation would remove the dependence of the PT on the distributions altogether. Therefore, control of the break-up process and monitoring the relation between the size distributions could be essential if as low as possible a PT is required for the envisaged nanocomposite application.

To that end, the use of a conductive penetrable ("soft") coating of the rodlike particles to effectively manipulate the hopping distance could be useful. In our model description of this we presume the effective hopping distance to be substantially increased by the coating, so that charge transport predominantly occurs via the intersection of either the coating and a particle or of two coatings. We find that a significant reduction of the PT can be gained by taking conductive instead of insulating particles if the fraction of coated rods is not very large. The conductive polymer latex PEDOT:PSS has been used as the coating material for the CNTs[21] and it was argued that the contribution of the CNTs could be neglected because the filler particles merely serve as a template for a percolating PEDOT:PSS network. However, we conclude that if the fraction of the particles without a coating is not negligible then neither is the conductivity of the CNTs. If the experiments are performed with insulating particles the mixture is nonadditive because charge transport is only possible between two coated particles and charge transport is blocked by any particle in a pair that has no coating. As a consequence, the PT is governed solely by the concentration of coated particles. By making the analogy with percolation on a Bethe lattice we demonstrated that this is because of the absence of loop correlations, which is a consequence of the use of the second-virial approximation that for slender rods should be accurate.[19]

In fact, it is instructive to evaluate the accuracy of this second-virial approximation. For this purpose we consider the following (virial) expansion for the direct pair connectedness function $\hat{C}^+$ at zero wave vector, $\hat{C}^+(0) = \hat{C}_2^+(0) + \rho\,\hat{C}_3^+(0) + \rho^2\hat{C}_4^+(0) + \ldots$, where $\hat{C}_n^+(0)$ denotes the n-body contribution, ρ denotes the number density, and angular averages are implied.[9,20,55] We refer to Appendix A for details. For rodlike particles we find that $\hat{C}_2^+ = \mathcal{O}(\lambda L^2)$ and $\hat{C}_3^+ = \mathcal{O}(\lambda^3 L^3)$, so $\hat{C}_3^+/(\hat{C}_2^+)^2 = \mathcal{O}(\lambda/L)$. This implies that the impact of the three-body virial is indeed negligibly small because the hopping distance λ is much smaller than the rod length L. A similar argument can be shown to hold for the higher-order terms, which justifies the truncation of the virial expansion after the first term, at least for rodlike particles. In practice, the approximation can be considered to be quantitative if $\langle L\rangle/\lambda > 100$, with $\langle L\rangle$ the mean length, and semiquantitative for $\langle L\rangle/\lambda > 20$.[28] Even the former, more strict condition, quite generally holds for individual CNTs, i.e., collections of exfoliated CNTs not dominated by bundles.

The central equations (10) and (11) of our theory apply to other types of particle, including spherical and platelike nanofillers. The latter may serve as a model for graphene. Unfortunately, for these the second-virial approximation should be expected to break down. Indeed, for both platelike and spherical particles of diameter D, we find that $\hat{C}_2^+ = \mathcal{O}(\lambda D^2)$ and $\hat{C}_3^+ = \mathcal{O}(\lambda D^5)$, both to leading order in λ/D. See also Appendix A. Hence, $\hat{C}_3^+/(\hat{C}_2^+)^2 = \mathcal{O}(D/\lambda)$, which is much larger than 1 for small hopping distances on the scale of the particle size. This means that the virials to all orders in the density should contribute to the PT for both types of particle. On the other hand, and rather surprisingly, it has been shown by means of Monte Carlo simulations that the second-virial approximation is reasonably accurate for spherical particles too, provided that the hopping distance is small relative to the particle size.[29] It is not clear why this is so but presumably this is caused by mutual cancellation of higher-order virials. It is reasonable to presume that this is also the case for platelike particles. Indeed, recent calculations show that the topologies of phase diagrams of binary mixtures of hard platelets of different sizes are the same for a second-virial theory and fundamental measure theory.[56] The latter is known to be highly accurate.

Because of this our model may within the second-virial approximation still give qualitative results for platelike particles, where we repeat that in this approximation of the pair-connectedness function P corrections to all orders in the density are included through linear graphs. We calculate $\hat{f}^+$ for hard polydisperse platelike particles[31] of thickness L and by following a similar procedure as for the rods, we find for the PT,

$$\phi_p = \frac{4\langle L_k D_\gamma^2\rangle_{k\gamma}\left(B - \sqrt{B^2 - C}\right)}{\lambda C}, \tag{24}$$

with

$$B = 4(\pi+5)\langle L_k D_\gamma\rangle_{k\gamma} + (5\pi+6)\langle D_\gamma^2\rangle_\gamma + (7\pi+16)\lambda\langle D_\gamma\rangle_\gamma, \tag{25}$$

$$C = (\pi+6)\Big(-16\pi\langle D_\gamma\rangle_\gamma\langle D_\gamma^3\rangle_\gamma - (\pi+6)\langle D_\gamma^4\rangle_\gamma + (17\pi+6)\langle D_\gamma^2\rangle_\gamma^2\Big). \tag{26}$$

Equation (24) holds provided $L, \lambda \ll D$ and provided L and λ are of the same order of magnitude. In the monodisperse limit, it reduces to $\phi_p = 2L/\lambda(5\pi+6)$, which, interestingly, is independent of the disk diameter D. This may seem surprising but if we again invoke our simple contact-volume argument as we did for the rodlike particles, we obtain a result consistent with it.[32] If we substitute typical values for

Downloaded 22 Mar 2011 to 131.155.110.244. Redistribution subject to AIP license or copyright; see http://jcp.aip.org/about/rights_and_permissions

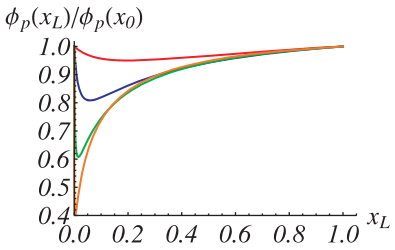

FIG. 7. The percolation threshold of a binary mixture of large (D_{large}) and small disks (D_{small}) of equal thickness is shown as a function of the mole fraction x_L of large plates relative to its value $\phi_p(x_0) = 2L/\lambda(5\pi + 6)$ of that of the corresponding monodisperse distribution with equal mean length. The tunneling distance λ is presumed to be a constant and drops out of the equation. From top to bottom: $D_{\text{large}}/D_{\text{small}} = 2, 4, 8$, and 16. The ratio of PTs is lowered substantially by adding a small fraction of large plates to a dispersion of small ones.

single-layer graphene, i.e., $L \approx 0.3$ nm and $\lambda \approx 1$ nm,[12] we find $\phi_p \approx 0.03$. This is (considerably) larger than experimental values of $10^{-4} - 10^{-2}$ found in the literature,[3,57,58] but the discrepancy may partly be explained by polydispersity effects and/or the influence of attractive interactions between them.[12] In spite of the PT being independent of the diameter in the monodisperse limit, the effect of diameter polydispersity is actually very strong, as is shown in Fig. 7. Similar to what we found to be the case of bidisperse rods in Fig. 3, adding a small quantity of wider sheets to any given collection lowers the PT and quite considerably so if they are sufficiently large relative to those already present in this collection. The effect wears off with increasing quantities, and our conjecture is that this is because while the small disks can form bridges between the large ones and have a relatively large freedom in their orientations, the large plates have are very restricted in their angular margin due to the excluded-volume interactions.

It appears that any kind of size bidispersity can have a large influence on the PT of a composite. To see if *shape* polydispersity has a similar impact, we also computed the percolation threshold for a mixture of rodlike and platelike particles to model a mixture of carbon nanotubes and graphene sheets. See also Fig. 8. For this we used the connectedness Mayer function $\hat{f}^+$ for the interactions between two rods and two plates as derived before, and computed that of the rod–plate interaction. If we solve Eq. (11), we find that for thin rods (say, SWCNTs) the lowest PT is obtained in a dispersion of only rods but for thicker rods (MWCNTs), adding a few plates becomes increasingly favorable albeit that the effect is modest. However, it must be noted that we presumed the rods and plates to exhibit cooperative connectivity behavior, i.e., the hopping distance between a rod and a plate equals that between two rods and between two plates, and this may be a tenuous approximation.[59]

Clearly, the central message that we obtain from our calculations is that connectivity percolation is a highly sensitive function of all thinkable system parameters. These include size, shape, connectivity, and any variation in and correlations between them. This suggests that in order to draw qualitative conclusions from experiments, complete control over, or at least a full description of these system parameters, is necessary. In this light it seems reasonable to suggest that the processing conditions leading up to the final nanocomposite must be as important as the properties of the nanofillers used in it. Hence, in the near future we aim to investigate the impact on the network formation of other aspects that play a role in the nanocomposite processing, including particle alignment and the equilibration of the network in the early stages of the cluster formation.

ACKNOWLEDGMENTS

The work of R.O. forms part of the research programme of the Dutch Polymer Institute (DPI, project 648). The authors thank Dr. Mark Miller, Dr. Tanja Schilling, Dr. Claudio Grimaldi, Dr. Cor Koning, Evgeniy Tkalya, Dr. Joachim Loos, and Marcos Ghislandi for stimulating discussions.

APPENDIX A: SECOND-VIRIAL APPROXIMATION

In order to assess the accuracy of the second-virial approximation for several particle shapes, we aim to compute the relative magnitude of the first and second terms in the density expansion of the Fourier transform of the direct pair connectedness function at zero wave vector $\hat{C}^+(0)$, $\hat{C}^+(0) = \hat{C}_2^+(0) + \rho\,\hat{C}_3^+(0) + \ldots$. Here, $\hat{C}_2^+$ and $\hat{C}_3^+$ are the

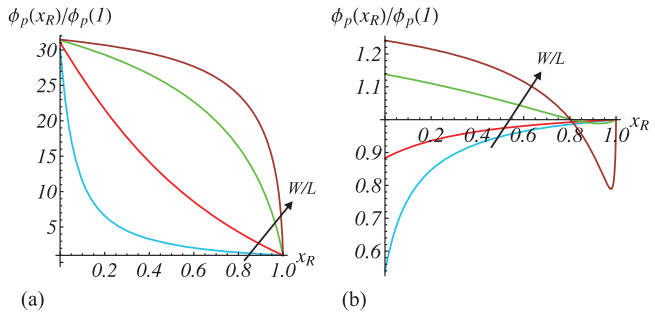

FIG. 8. For a bidisperse mixture of plates with diameter W and thickness T and rods with length L and diameter D, the percolation threshold ϕ_p relative to its value of that of the corresponding monodisperse case consisting of only rods is shown as a function of the mole fraction x_R of rods. The arrows indicate increasing values of W/L: 0.1, 0.3, 1 and 3. (a) For typical values for graphene and CNTs, $L/T = 1500$ and $L/\lambda = L/D = 500$, where λ is the hopping distance, a mixture with only rods gives the lowest PT. For sufficiently large rod aspect ratios L/D, the shape of the curves is almost insensitive to changes in L/T and L/λ, which only change the vertical scale. (b) For rods with a smaller L/D, a mixture with plates can have a lower PT than the one for only rods, as shown for $L/T = 60$, $L/\lambda = L/D = 15$.

Downloaded 22 Mar 2011 to 131.155.110.244. Redistribution subject to AIP license or copyright; see http://jcp.aip.org/about/rights_and_permissions

two-body and three-body direct connectedness functions, and we omit the arguments $\mathbf{u}$ and $\mathbf{u}'$ for notational convenience. In order to compare the third virial term with the second, we note that for the critical number density of particles at the PT ρ_p, we have $\rho_p \langle \hat{C}^+(0)\rangle_{\mathbf{u},\mathbf{u}'} \approx 1$.[9,20] If we truncate the virial expansion after $\hat{C}_3^+$, we have $\rho_p \hat{C}_2^+(0) + \rho_p^2 \hat{C}_3^+(0) = 1$. This gives

$$\rho_p \langle \hat{C}_2^+(0)\rangle_{\mathbf{u},\mathbf{u}'} \left(1 + \rho_p \frac{\langle \hat{C}_3^+(0)\rangle_{\mathbf{u},\mathbf{u}'}}{\langle \hat{C}_2^+(0)\rangle_{\mathbf{u},\mathbf{u}'}}\right) = 1, \tag{A1}$$

so the second-virial approximation is valid if $\langle \hat{C}_3^+(0)\rangle_{\mathbf{u},\mathbf{u}'} / \langle \hat{C}_2^+(0)\rangle_{\mathbf{u},\mathbf{u}'}^2 \ll 1$. To evaluate $\hat{C}_3^+(0)$, we follow the approach introduced by Coniglio *et al.*[20] According to their definition, $C_n^+(\mathbf{r}, \mathbf{r}', \mathbf{u}, \mathbf{u}')$ contains all graphs (diagrams) consisting of n points in a diagrammatic expansion with at least one continuous path of f^+ bonds between the two particles at $\mathbf{r}$ and $\mathbf{r}'$, so they are part of the same cluster and interact via a potential u^+. Particles that are not directly connected within the same cluster are said to be "connected" by an f^* bond and interact via the potential u^*. This bond is defined as $f^* \equiv \exp(-\beta u^*) - 1$, such that $f \equiv f^+ + f^*$ is the Mayer function with $\exp(-\beta u^+) + \exp(-\beta u^*) = \exp(-\beta u) = f + 1$.[60] We consider hard particles in the cherry-pit model, so $f^+ = 1$ for $D < r < \Delta$ and $f^+ = 0$ otherwise, with r being the distance between the particles, so it is nonzero only if two particles are connected, i.e., if their connectedness zones overlap. For f^* we have $f^* = -1$ for $r < \Delta$ and $f^* = 0$ for $r > \Delta$, meaning that f^* is nonzero if the particles either intersect or if they are connected. Furthermore, $f = f^+ + f^*$, which equals -1 for $r < D$, i.e., particle intersection, and zero otherwise.

For the second virial coefficient $\hat{C}_2^+$, the diagrams consist only of the points 1 and 2, so only the one with an f^+ bond between these points meets the criterion and $\hat{C}_2^+(0, \mathbf{u}, \mathbf{u}') = \int f^+(\mathbf{r}_{12}) d\mathbf{r}_{12}$, with $\mathbf{r}_{12} = \mathbf{r}_2 - \mathbf{r}_1$, which is the contact volume for particles that can be obtained from the excluded volume for cylindrical particles of length L and diameter D.[31] In the case of rodlike particles in an additive system, this gives Eq. (13), so $\hat{C}_2^+(0, \mathbf{u}, \mathbf{u}') = 2L^2\lambda|\sin\gamma|$ for a constant rod length L and hopping distance λ and where γ is the angle between the orientations $\mathbf{u}$ and $\mathbf{u}'$. For platelike particles the excluded volume gives to leading order for large aspect ratios $\hat{C}_2^+(0, \mathbf{u}, \mathbf{u}') = \frac{3}{2}\pi D^2\lambda|\sin\gamma|$, with D being the disk diameter.

For the third virial coefficient we can form five diagrams, shown in Fig. 9, that meet Coniglio's criterion,[55] which then gives

$$\hat{C}_3^+(0, \mathbf{u}, \mathbf{u}') = \int\int \left(f_{12}^+ f_{13}^+ f_{23}^+ + f_{12}^+ f_{13}^+ f_{23}^* + f_{12}^+ f_{13}^* f_{23}^+ + f_{12}^* f_{13}^+ f_{23}^+ + f_{12}^+ f_{13}^* f_{23}^*\right) d\mathbf{r}_{12} d\mathbf{r}_{13}. \tag{A2}$$

To compute this integral we note that $f^* = -1$, if the two particles either intersect or if they are connected, which can be subdivided into the intersection ($f = -1$) and the connection ($f = +1$). We can thus replace f^+ by c and f^* by $s - c$, where c and s indicate a configuration where two particles are connected and intersect, respectively. We then find $\hat{C}_3^+(0, \mathbf{u}, \mathbf{u}') = -c^3 + c^2 s + cs^2$, so we have to compute the

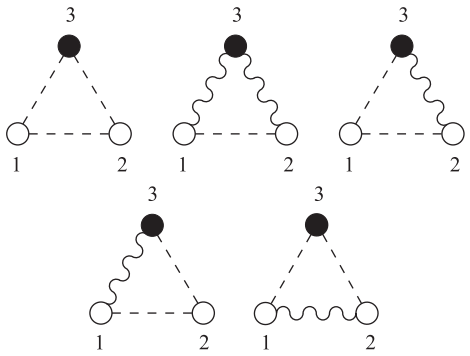

FIG. 9. Five diagrams consisting of three points can be formed such that points 1 and 2 are connected via a continuous path of f^+ bonds (dashed lines), where the wavy lines represent f^* bonds. This path between 1 and 2 can be either direct, as in the top three and the bottom left diagram, or via a third particle, shown by the bottom right diagram. These diagrams give rise to the five terms in the expression (A2) for $\hat{C}_3^+(0, \mathbf{u}, \mathbf{u}')$.

"volume" of a configuration where the three particles are mutually connected, one where two contacts are connections in the overlap zone and the third is an intersection, and one with two intersections and one connection.

For rodlike particles we obtain the following estimate for the order of magnitude of the different terms. The configuration in which the three particles are mutually connected gives λL^2 for the first contact between two rods, ignoring a constant of the order unity. The third rod needs to be connected to both other rods, which gives an additional volume proportional to λL^2 it can occupy, but it has only a very small angle of the order λ/L that it can move, which then gives $\lambda^3 L^3$ in total. The second and third terms $cs(s + c)$ can be combined by starting again with two connected rods, giving λL^2 for the c. The third particle then has to intersect one of the first two (a factor D from the s), it has to intersect or make contact with the other (a factor $D + \lambda$ from the $s + d$), and then has a freedom L in the third direction. So we find for this contribution $\lambda D(D + \lambda)L^3$. For SWCNTs, D is probably larger than λ and for MWCNTs it is much larger, so the third virial term is of the order $\lambda D^2 L^3$. Its relative magnitude is then $\lambda D^2 L^3/(\lambda L^2)^2 = D^2/\lambda L \ll 1$ because $L \ll D$, and the second-virial approximation is accurate for rodlike particles.

For platelike particles the situation turns out to be quite different. From a similar argument as that for the rods we find that the c^3 term gives a contribution to $\hat{C}_3^+$ of the order $\lambda^3 D^3$, where D now denotes the disk diameter. The way this estimate is obtained is explained in Fig. 10. We again take the terms $c^2 s$ and cs^2 together, so the two connected plates give λD^2 for the c. The third particle then intersects the first, giving a D, is either connected to the second or intersects it, giving a $D + \lambda$, and has the freedom to move a distance D in the third direction. Hence, for these terms we find a contribution $\lambda(D + \lambda)D^4 \approx \lambda D^5$, which is much larger than the first term from the three mutually connected disks. Compared to the second virial term, its magnitude is $\lambda D^5/(\lambda D^2)^2 = D/\lambda$ that is much larger than unity and would make the truncation of the virial expansion of $\hat{C}^+$ after the first term unjustified. The scaling for spherical particles gives similar results for $\hat{C}_2^+$ and $\hat{C}_3^+$, where D then denotes the sphere diameter. So for

Downloaded 22 Mar 2011 to 131.155.110.244. Redistribution subject to AIP license or copyright; see http://jcp.aip.org/about/rights_and_permissions

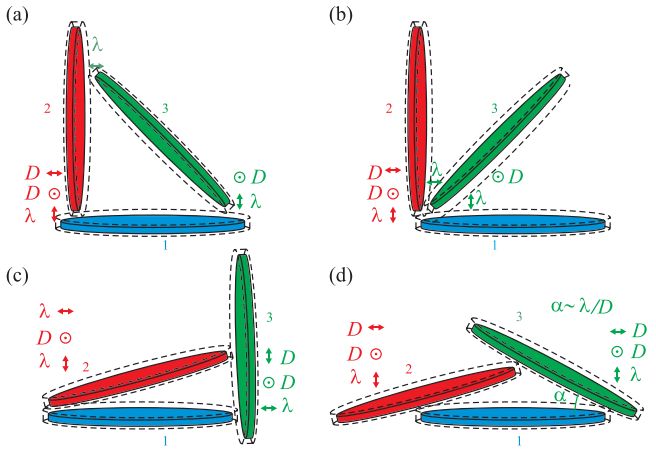

FIG. 10. Possible configurations of three disks that are mutually connected and that contribute to the three-body direct connectedness function $\hat{C}_3^+(0)$. The disks have diameter D and the tunneling distance between them is $\lambda \ll D$. If we fix disk 1 and if the difference between the orientations of disk 1 and 2 are almost perpendicular to each other, the overlap criterion is met in a triangle (a) or a branched configuration (b). If this difference is very small, on the other hand, we distinguish between almost complete (c) and limited overlap (d) between particles 1 and 2. In the latter case the angle α that disks 2 and 3 make is of the order λ/D. λ and D denote the ranges of motion in three directions for the disk 2 so that it is connected to disk 1 and for the disk 3 so that it connects to 1 and 2. In all cases we find $\hat{C}_3^+(0) = \mathcal{O}(\lambda^3 D^3)$.

spheres the second-virial approximation would not be suitable either, but it turns out not to be very inaccurate if $\lambda \ll D$,[29] possibly because of mutual cancellation of higher-order virials.

APPENDIX B: SYMMETRIC LENGTH DISTRIBUTIONS

We consider symmetric distributions, i.e., with zero skewness, to compute the maximum effect the spread in the length distribution can have on the PT, i.e., the largest value of s in $\phi_p(x)/\phi_p(x_0) = 1/(s+1)$ that was derived in Sec. III. For a truly symmetric distribution we can write

$$\langle L_k \rangle_k = \frac{1}{2}(L_{\text{long}} + L_{\text{short}}), \tag{B1}$$

with L_{long} (L_{short}) being the length of the longest (shortest) rod in the distribution.[61] It follows that in that case the largest value of $s = \text{Var}(L_k)/\langle L_k \rangle_k^2 = 4\text{Var}(L_k)/(L_{\text{long}} + L_{\text{short}})^2$ for given L_{long} and L_{short} is obtained for a distribution with all L_k taking either the value L_{long} or L_{short}, because any rod with a length larger than L_{short} or smaller than L_{long} would lower $\text{Var}(L_k)$. Obviously, the number of rods with length L_{long} and L_{short} must be equal to make the distribution symmetric. This then implies that a bidisperse distribution with a probability density

$$f(L) = \frac{1}{2}\delta(L - L_{\text{long}}) + \frac{1}{2}\delta(L - L_{\text{short}}), \tag{B2}$$

with δ being the familiar Dirac delta function, produces the largest value of s feasible for symmetric distributions. If we write $L_{\text{long}} = nL_{\text{short}}$ with n being a real number larger than unity, as we did for the bidisperse mixtureM in Fig. 3, we find $\text{Var}(L_k) = L_{\text{short}}^2(n^2-1)/4$, and $\langle L_k \rangle_k = \frac{1}{2}L_{\text{short}}(n+1)$, and

$$s = \frac{(n-1)^2}{(n+1)^2}. \tag{B3}$$

Expression (B3) for s is a monotonically increasing function of n and has a *maximum* value of 1 in the limit of $n \to \infty$, i.e., an infinite length ratio. With $\phi_p(x)/\phi_p(x_0) = 1/(s+1)$ this means that the reduction of the PT that can be obtained with a symmetric length distribution is *at most* a factor 2 relative to that of the monodisperse case, denoted by x_0, and achieved for the limit $L_{\text{short}} \to L_{\text{long}}$.

[1] K. S. Novoselov, A. K. Geim, S. V. Morozov, D. Jiang, Y. Zhang, S. V. Dubonos, I. V. Grigorieva, and A. A. Firsov, Science **306**, 666 (2004).
[2] M. Moniruzzaman and K. I. Winey, Macromolecules **39**, 5194 (2006).
[3] S. Stankovich, D. A. Dikin, G. H. B. Dommett, K. M. Kohlhaas, E. J. Zimney, E. A. Stach, R. D. Piner, S. T. Nguyen, and R. S. Ruoff, Nature (London) **442**, 282 (2006).
[4] D. Stauffer and A. Aharony, *Introduction to Percolation Theory* (Taylor & Francis, London, 1992).
[5] N. Grossiord, J. Loos, O. Regev, and C. E. Koning, Chem. Mater. **18**, 1089 (2006).
[6] E. J. Garboczi, K. A. Snyder, J. F. Douglas, and M. F. Thorpe, Phys. Rev. E **52**, 819 (1995).
[7] I. Balberg, C. H. Anderson, S. Alexander, and N. Wagner, Phys. Rev. B **30**, 3933 (1984).
[8] I. Balberg, Phys. Rev. B **33**, 3618 (1986).
[9] A. L. R. Bug, S. A. Safran, and I. Webman, Phys. Rev. B **33**, 4716 (1986).
[10] A. Celzard E. McRae, C. Deleuze, M. Dufort, G. Furdin, and J. F. Mareche, Phys. Rev. B **53**, 6209 (1996).
[11] K. Leung and D. Chandler, J. Stat. Phys. **63**, 837 (1991).
[12] A. V. Kyrylyuk and P. van der Schoot, Proc. Natl. Acad. Sci. U.S.A. **105**, 8221 (2008).
[13] Y. R. Hernandez, A. Gryson, F. M. Blighe, M. Cadek, V. Nicolosi, W. J. Blau, Y. K. Gunko, and J. N. Coleman, Scr. Mater. **58**, 69 (2008).
[14] P. Sollich, J. Phys.: Condens. Matter **14**, R79 (2002).
[15] K. Shundyak, R. van Roij, and P. van der Schoot, J. Chem. Phys. **122**, 094912 (2005).
[16] As produced graphene sheets are conductive but if they are first oxidized and later reduced in the processing of the nanocomposites, their conductivity can be strongly reduced. See also Ref. 57.
[17] H. Deng, R. Zhang, E. Bilotti, J. Loos, and A. A. J. M. Peijs, J. Appl. Polym. Sci. **113**, 742 (2009).
[18] J. P. Hansen and I. MacDonald, *Theory of Simple Liquids*, 2nd ed. (Academic, London, 1986).
[19] R. H. J. Otten and P. van der Schoot, Phys. Rev. Lett. **103**, 225704 (2009).
[20] A. Coniglio, U. De Angelis, and A. Forlani, J. Phys. A **10**, 1123 (1977).
[21] M. C. Hermant, B. Klumperman, A. V. Kyrylyuk, P. van der Schoot, and C. E. Koning, Soft Matter **5**, 878 (2009).
[22] S. I. White, R. M. Mutiso, P. M. Vora, D. Jahnke, S. Hsu, J. M. Kikkawa, J. Li, J. E. Fischer, and K. I. Winey Adv. Funct. Mater. **20**, 2709 (2010).
[23] G. Stell, Physica A **231**, 1 (1996).
[24] R. Fantoni, D. Gazzillo, and A. Giacometti, J. Chem. Phys. **122**, 034901 (2005).
[25] A. P. Chatterjee, J. Phys.: Condens. Matter **20**, 255250 (2008).
[26] S. Torquato, *Random Heterogeneous Materials: Microstructure and Macroscopic Properties* (Springer, New York, 2002).
[27] In fact, P and C^+ can be expressed in terms of a sum of graphs and describe average probabilities of having the particles connected in such a graph, which is not an actual cluster.
[28] G. J. Vroege and H. N. W. Lekkerkerker, Rep. Prog. Phys. **55**, 1241 (1992).
[29] T. DeSimone, S. Demoulini, and R. M. Stratt, J. Chem. Phys. **85**, 391 (1986).
[30] J. P. Straley, Phys. Rev. A **8**, 2181 (1973).
[31] L. Onsager, Ann. N. Y. Acad. Sci. **51**, 627 (1949).
[32] G. Ambrosetti, C. Grimaldi, I. Balberg, T. Maeder, A. Danani, and P. Ryser, Phys. Rev. B **81**, 155434 (2010).
[33] M. C. Hermant, P. van der Schoot, B. Klumperman, and C. E. Koning, ACS Nano **4**, 2242 (2010).

Downloaded 22 Mar 2011 to 131.155.110.244. Redistribution subject to AIP license or copyright; see http://jcp.aip.org/about/rights_and_permissions

[34]F. Dalmas, R. Dendievel, L. Chazeau, J.-Y. Cavaillé, and C. Gauthier, Acta Mater. **54**, 2923 (2006).
[35]A. P. Chatterjee, J. Chem. Phys. **132**, 224905 (2010).
[36]In probability theory, $\sqrt{s} = \sqrt{\mathrm{Var}(L_i)}/\langle L_i\rangle_i$ is called the coefficient of variation (or variation coefficient) of the distribution of L_i. See also Ref. 45.
[37]C. Lu and J. Liu, J. Phys. Chem. B **110**, 20254 (2006).
[38]C. L. Cheung, A. Kurtz, H. Park, and C. M. Lieber, J. Phys. Chem. B **106**, 2429 (2002).
[39]T. Yamada, T. Namai, K. Hata, D. N. Futaba, K. Mizuno, J. Fan, M. Yudasaka, M. Yumura, and S. Iijima, Nat. Nanotechnol. **1**, 131 (2006).
[40]S. Wang, Z. Liang, B. Wang, and C. Zhang, Nanotechnology **17**, 634 (2006).
[41]J. Li and J.-K. Kim, Compos. Sci. Technol. **67**, 2114 (2007).
[42]A. F. Holloway, D. A. Craven, L. Xiao, J. Del Campo, and G. G. Wildgoose, J. Phys. Chem. C **112**, 13729 (2008).
[43]A. S. Berdinsky, P. S. Alegaonkar, H. C. Lee, J. S. Jung, J. H. Han, J. B. Yoo, D. Fink, and L. T. Chadderton, NANO **2**, 59 (2007).
[44]A. N. G. Parra-Vasquez, I. Stepanek, V. A. Davis, V. C. Moore, E. H. Haroz, J. Shaver, R. H. Hauge, R. E. Smalley, and M. Pasquali, Macromolecules **40**, 4043 (2007).
[45]R. V. Hogg and A. T. Craig, *Introduction to Mathematical Statistics*, 4th ed. (Macmillan, New York, 1978).
[46]The skewness $\gamma \equiv \langle (L_i - \langle L_i\rangle_i)^3\rangle_i / \langle (L_i - \langle L_i\rangle_i)^2\rangle_i^{3/2}$ need not go to zero in the monodisperse limit, because both the numerator and the denominator go to zero and the speed of convergence of both determines the monodisperse value of γ.
[47]*Handbook of Mathematical Functions with Formulas, Graphs, and Mathematical Tables*, edited by M. Abramowitz, I. A. Stegun, and Irene (Dover Publications, New York, 1972).
[48]Á. Kukovecz, T. Kanyó, and Z. Kónya, I. Kiricsi, Carbon **43**, 994 (2005).
[49]A. Lucas, C. Zakri, M. Maugey, M. Pasquali, P. van der Schoot, and P. Poulin, J. Phys. Chem. C **113**, 20599 (2009).
[50]G.-H. Jeong, S. Suzuki, Y. Kobayashi, A. Yamazaki, H. Yoshimura, and Y. Homma, J. Appl. Phys. **98**, 124311 (2005).
[51]M. S. Arnold, A. A. Green, J. F. Hulvat, S. I. Stupp, and M. C. Hersam, Nat. Nanotechnol. **1**, 60 (2006).
[52]B. Yu, P.-X. Hou, F. Li, B. Liu, C. Liu, and H.-M. Cheng, Carbon **48**, 2941 (2010).
[53]This requires the conductive layer to be above its glass temperature in the preparatory phase in the production stages of the composite. This in practice is the case. See Ref. 21.
[54]E. T. Thostenson and T.-W. Chou, J. Phys. D: Appl. Phys. **35**, L77 (2002).
[55]R. Fantoni, D. Gazzillo, A. Giacometti, M. A. Miller, and G. Pastore, J. Chem. Phys. **127**, 234507 (2005).
[56]J. Phillips and M. Schmidt, Phys. Rev. B **81**, 041401 (2010).
[57]E. Tkalya, M. Ghislandi, A. Alekseev, C. Koning, and J. Loos, J. Mater. Chem. **20**, 3035 (2010).
[58]H.-B. Zhang, W.-G. Zheng, Q. Yan, Y. Yang, J.-W. Wang, Z.-H. Lu, G.-Y. Ji, and Z.-Z. Yu, Polymer **51** 1191–1196 (2010).
[59]A. V. Kyrylyuk, M. C. Hermant, T. Schilling, B. Klumperman, C. E. Koning, and P. van der Schoot, "Controlling electrical percolation in multicomponent carbon nanotube dispersions," Nature Nanotechnology (to be published).
[60]T. L. Hill, J. Chem. Phys. **23**, 617 (1955).
[61]For a Gaussian distribution centered around $\langle L_k\rangle_k$ this is not strictly the case because by definition $L_k > 0$; however, for $s \ll 1$ it becomes approximately true with $L_{\mathrm{short}} = 0$ and $L_{\mathrm{long}} = 2\langle L_k\rangle_k$.

Downloaded 22 Mar 2011 to 131.155.110.244. Redistribution subject to AIP license or copyright; see http://jcp.aip.org/about/rights_and_permissions